Stem Cell Reports
Article
OPEN ACCESS

# Temporal Perturbation of the Wnt Signaling Pathway in the Control of Cell Reprogramming Is Modulated by TCF1

Francesco Aulicino,[1,2,4] Ilda Theka,[1,2,4] Luigi Ombrato,[1,2] Frederic Lluis,[1,2,5,*] and Maria Pia Cosma[1,2,3,5,*]
[1]Centre for Genomic Regulation (CRG), Dr. Aiguader 88, 08003 Barcelona, Spain
[2]Universitat Pompeu Fabra (UPF), 08003 Barcelona, Spain
[3]Institució Catalana de Recerca i Estudis Avançats (ICREA), Pg. Lluis Companys 23, 08010 Barcelona, Spain
[4]These authors contributed equally to this work
[5]These authors contributed equally to this work
*Correspondence: frederic.lluis@crg.es (F.L.), pia.cosma@crg.es (M.P.C.)
http://dx.doi.org/10.1016/j.stemcr.2014.04.001


## SUMMARY

Cyclic activation of the Wnt/β-catenin signaling pathway controls cell fusion-mediated somatic cell reprogramming. TCFs belong to a family of transcription factors that, in complex with β-catenin, bind and transcriptionally regulate Wnt target genes. Here, we show that Wnt/β-catenin signaling needs to be off during the early reprogramming phases of mouse embryonic fibroblasts (MEFs) into iPSCs. In MEFs undergoing reprogramming, senescence genes are repressed and mesenchymal-to-epithelial transition is favored. This is correlated with a repressive activity of TCF1, which contributes to the silencing of Wnt/β-catenin signaling at the onset of reprogramming. In contrast, the Wnt pathway needs to be active in the late reprogramming phases to achieve successful reprogramming. In conclusion, continued activation or inhibition of the Wnt/β-catenin signaling pathway is detrimental to the reprogramming of MEFs; instead, temporal perturbation of the pathway is essential for efficient reprogramming, and the "Wnt-off" state can be considered an early reprogramming marker.

## INTRODUCTION

The activation of canonical Wnt/β-catenin pathway controls embryo development and early differentiation events (MacDonald et al., 2009). However, it can also control the self-renewal and pluripotency of stem cells (Kühl and Kühl, 2013; Sato et al., 2004; Sokol, 2011). The activation of this pathway is due to the inhibition of the β-catenin destruction complex formed by APC, GSK3, and AXIN, resulting in β-catenin stabilization. Consequently, β-catenin can then translocate into the nucleus and activate target genes via its association with the TCF factors (Cadigan and Liu, 2006; Hoppler and Kavanagh, 2007; Moon et al., 2004). TCF proteins belong to a family of transcription factors, which include TCF1, LEF1, TCF3, and TCF4. TCF1 and LEF1 can bind β-catenin and activate target genes when the Wnt pathway is active (Hoppler and Kavanagh, 2007; Hurlstone and Clevers, 2002; Willert and Jones, 2006). In contrast, when the Wnt pathway is not active, all the TCF factors can recruit repressive complexes and function as repressors of target genes (Brantjes et al., 2001; Daniels and Weis, 2005).

Embryonic stem cells (ESCs) cultured in 2i medium, which contains GSK3 and MEK inhibitors, can be propagated in a pluripotent ground state (Silva et al., 2008). Pluripotent ground state is also established by *Tcf3* deletion in ESCs (Cole et al., 2008; Tam et al., 2008; Wray et al., 2011; Yi et al., 2008, 2011). It is interesting to note that the GSK3 inhibitor in 2i medium stabilizes β-catenin. This suggests that the pluripotent ground state of ESCs can be maintained by derepression of TCF3 but also by activation of the Wnt pathway via stabilization of β-catenin. Moreover, activation of Wnt signaling prevents differentiation of ESCs into epiblast stem cells (epiSCs), through regulation of the transition between the ground and primed states (ten Berge et al., 2011).

The Wnt/β-catenin pathway can also activate somatic cell reprogramming to pluripotency. Mouse embryonic fibroblasts (MEFs) transduced with retroviruses carrying *Oct4*, *Klf4*, and *Sox2* and cultured in medium containing Wnt3a can generate induced pluripotent stem cell (iPSC) colonies with enhanced efficiency in absence of *c-Myc* (Marson et al., 2008). Furthermore, activation of the Wnt pathway in ESCs enables them to reprogram neural precursor cells after fusion (Lluis et al., 2008). Finally, the deletion of *Tcf3* greatly enhances cell-fusion-mediated reprogramming, as well as the production of induced pluripotent stem cells (iPSCs) (Lluis et al., 2011; Ombrato et al., 2012).

In addition to the Wnt-mediated control of ESC pluripotency and somatic cell reprogramming, Wnt signaling is also a driver of differentiation during early developmental phases (Tam and Loebel, 2009). Anterior-posterior axis specification in the mouse embryo occurs through the activity of Wnt signaling (Merrill et al., 2004; Sokol, 2011). In particular, Wnt signaling activity is essential for establishment of the primitive streak and anterior-posterior polarity, i.e., for epithelial-to-mesenchymal transition of epiblast cells in the primitive streak (Kalluri and Weinberg, 2009; Murry and Keller, 2008; Tanaka et al., 2011; ten Berge et al., 2008).

These apparently opposite roles of the Wnt signaling pathway are therefore a conundrum; on one hand, Wnt activity controls ESC pluripotency, and on the other hand, it regulates early developmental differentiation events. To reconcile these opposite functions, one reasonable hypothesis is based on the level of activation of the Wnt pathway in time. It is well known that Wnt signaling oscillates during development and that its target genes have an oscillatory behavior (Sokol, 2011; van Amerongen and Nusse, 2009). At the same time, cyclic activation of the Wnt/β-catenin pathway is essential for enhancing somatic cell reprogramming (Lluis and Cosma, 2009; Lluis et al., 2008). If β-catenin activity is either high or very low, reprogramming does not take place. We therefore wondered whether the activation of Wnt signaling activity mediated by TCF factors is essential in a specific phase of the reprogramming of MEFs into iPSCs.

TCF3 and TCF1 share a similar DNA binding domain, and they represent the most highly expressed TCF family factors in ESCs (Lluis et al., 2011; Pereira et al., 2006). TCF3 acts as a repressor of Wnt target genes, and in contrast TCF1 can activate or repress Wnt-targets via its association with β-catenin (Brantjes et al., 2001; Hikasa et al., 2010). However, little is known about TCF1 function in ESCs, and here we investigated the role of TCF1 in the reprogramming process of MEFs into iPSCs. Surprisingly, in this context, we found that the activity of the Wnt/β-catenin pathway needs to be switched off during the first days and that the cells undergoing reprogramming have low levels of stabilized β-catenin. Remarkably, sorted Wnt "off" MEFs generate a very high number of NANOG-positive iPSCs. Interestingly, during the early phases of four-factor-induced reprogramming, TCF1 functions as a repressor of Wnt signaling, and this activity correlates with downregulation of senescent genes, such as *p21*, *p19*, and *p16*, and activation of mesenchymal-to-epithelial transition (MET) genes. The activity of the Wnt/β-catenin pathway is instead necessary during the late phases of the reprogramming process.

## RESULTS

### TCF1 Does Not Control Self-Renewal or Differentiation of ESCs

TCF3 is a repressor of pluripotency in ESCs, and its deletion drives the ESCs into a pluripotent ground state (Wray et al., 2011; Yi et al., 2011). Silencing of *Tcf1* does not affect ESC self-renewal (Yi et al., 2011). Here, we investigated whether TCF1 has a role in controlling mouse ESC differentiation. With this aim, we silenced *Tcf1* in ESCs by infecting the cells with two different lentiviral vectors that carry short hairpins for *Tcf1* (ESCs-shTcf1A, ESCs-shTcf1B) (Figures S1A and S1B available online) and observed that Wnt signaling activity was impaired (Figure S1C). The Wnt signaling activity was measured after activating the pathway with the GSK3 inhibitor BIO in ESCs-shTcf1A, ESCs-shTcf1B, and ESCs-shScr, which were previously infected with a lentivirus carrying the 7xTcf-eGFP reporter (7TGP) for TCF/β-catenin activity (Figure S1C) (Fuerer and Nusse, 2010). The reporter allowed the measurement of GFP as a Wnt signaling activation readout (Fuerer and Nusse, 2010). The viruses carrying the short hairpins also carried a hygromicin selection cassette, to allow the selection of the infected cells. Then we analyzed the expression of stem cell genes and self-renewal in ESCs-shTcf1A and ESCs-shTcf1B (Figure 1A). Expression of *Nanog*, *Stella*, and *Oct4* was not decreased after silencing of *Tcf1*, with respect to cells infected with a virus carrying a scrambled short hairpin (ESCs-shScr), which indicated that the expression of stem cell factors was not affected (Figure 1A). Finally, we performed clonogenic assays by culturing the same number of ESCs infected with shTcf1A, shTcf1B, and shScr and counting the number of alkaline-phosphatase-positive ($AP^+$) colonies, as a marker of pluripotency. The same number of colonies was counted under all three conditions, and their morphologies were indistinguishable (Figure 1B).

Next, we analyzed the possible defects in the differentiation potential of ESCs silenced for *Tcf1*. For this, we generated embryoid bodies using ESCs-shScr, ESCs-shTcf1A, and ESCs-shTcf1B. We analyzed the expression of pluripotent genes and of mesoderm, ectoderm, and endoderm markers at 3, 5, 7, and 9 days during embryoid body development. Embryoid bodies from both ESCs-shScr and ESCs-shTcf1A developed with the expected morphology at all time points analyzed (Figure 1C). Pluripotency genes, such as *Oct4*, *Nanog*, and *Rex1*, decreased with the same efficiency and kinetics in both the ESCs-shScr and ESCs-shTcf1A embryoid bodies. Furthermore, the mesoderm markers *Brachyury* and *Flk1*, the ectoderm markers *Fgf5* and *Pax6*, and the endoderm markers *Gata4* and *Foxa2* were expressed with the expected timing at 3, 5, 7, and 9 days of both ESCs-shScr and ESCs-shTcf1A embryoid body development (Figure 1D). Comparable efficiency of the differentiation potential was also obtained after analyzing the expression of pluripotent genes and of the mesoderm, ectoderm, and endoderm markers during embryoid body development for ESCs-shScr and ESCs-shTcf1B (Figures S1D and S1E).

In all, these data clearly show that silencing of *Tcf1* in mouse ESCs impairs neither self-renewal nor differentiation potential.

### Continuous *Tcf1* Silencing Impairs Reprogramming of MEFs to Pluripotency

Previous studies, including our own, have shown that the activation of Wnt signaling enhances cell-fusion-mediated

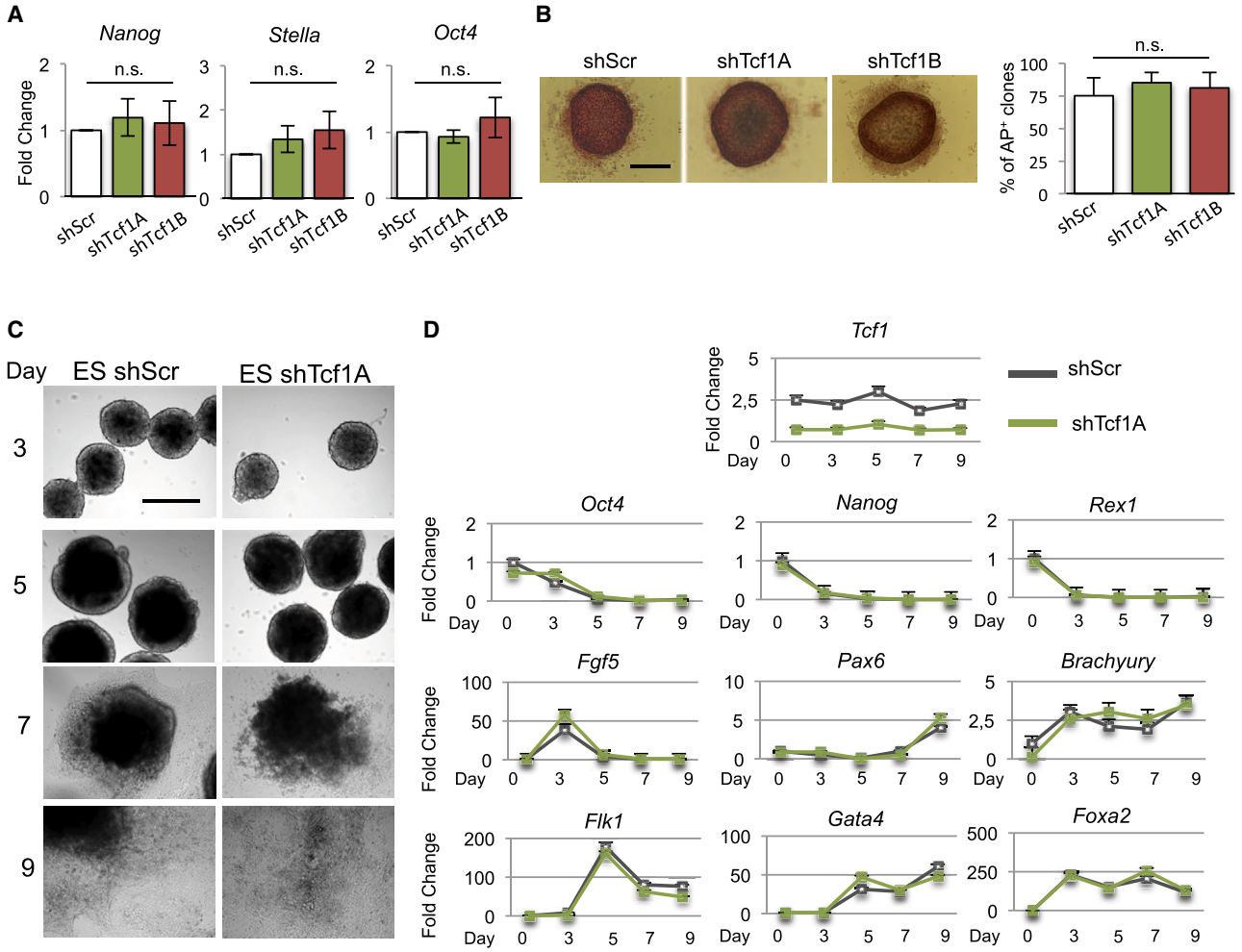


**Figure 1. Silencing of *Tcf1* in Mouse ESCs Does Not Affect Pluripotency**

(A) Quantitative PCR expression analysis of pluripotent markers *Nanog*, *Stella*, and *Oct4* in ESCs infected with lentiviruses carrying shScr or shTcf1A/B, as indicated. (n = 3, independent experiments).

(B) Representative colonies of ESCs-shScr and ESCs-shTcf1A/B showing alkaline phosphatase staining (left panels). Quantification on the right shows percentages of alkaline-phosphatase-positive ($AP^+$) colonies with respect to all ($AP^+$ and $AP^-$) colonies (n = 3 independent experiments). Scale bar, 300 μm.

(C) ESCs-shScr and ESCs-shTcf1A were subjected to differentiation through aggregation into embryoid bodies. Representative phase-contrast images at 3, 5, 7, and 9 days during embryoid body differentiation. Scale bar, 400 μm.

(D) Representative quantitative real-time PCR experiment (out of three independent experiments) for the detection of *Tcf1*, stem cell (*Oct-4*, *Nanog*, and *Rex1*), ectoderm (*Fgf5*, *Pax6*), mesoderm (*Brachyury*, *Flk1*), and endoderm (*Gata4* and *Foxa2*) marker genes in embryoid bodies at different times pi. The levels are normalized to *Gapdh*.

All pooled data are represented as means ± SD. See also Figure S1.

reprogramming of somatic cells to pluripotency and the efficiency of generation of iPSCs in the absence of c-Myc (Lluis et al., 2008; Marson et al., 2008). Furthermore, derepression of *Tcf3* greatly enhances the reprogramming efficiency of neural precursor cells to pluripotency (Lluis et al., 2011). We were next interested in studying the function of TCF1 in the control of somatic cell reprogramming. In addition, because TCF1 controls target genes through its association with β-catenin, in parallel, we investigated β-catenin activity in the regulation of reprogramming.

Thus, we infected doxycycline-inducible four-factor (*Oct4*, *Klf4*, *Sox2*, and *c-Myc*) MEFs (Carey et al., 2010) with shTcf1A, with shTcf1B, with shβ-catenin (shβ-cat), and with control shScr (Figures S2A and S2B). Infected MEFs were selected with hygromycin, replated at equal numbers, and subsequently induced with doxycycline for

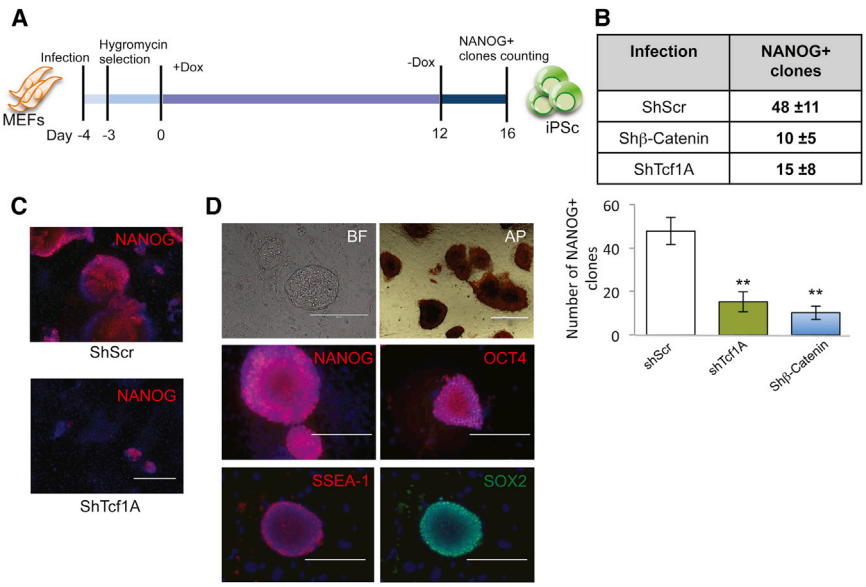


**Figure 2. Silencing of *Tcf1* in Four-Factor-Induced MEFs Impairs Reprogramming**

(A) Experimental scheme for iPSC generation. Four-factor MEFs were infected with lentiviral vectors carrying shScr, shTcf1A, and shβ-catenin. Infected cells were hygromycin selected for 3 days. Doxycycline was applied from 0 to 12 days, to activate expression of *Oct4*, *Klf4*, *Sox2*, and *c-Myc*. Then doxycycline was removed, and cells were allowed to grow for 4 days. At day 16, immunostaining against NANOG was performed, to count the number of reprogrammed clones.

(B) Number of NANOG-positive (NANOG$^+$) clones obtained according to each treatment, as indicated (n = 4 independent experiments).

(C) Representative image of a NANOG$^+$ clone obtained from shScr- and shTcf1-infected MEFs analyzed at day 16.

(D) Images of immunostaining of iPSC clones obtained from four-factor MEFs infected with shScr. Scale bars, 200 μm (NANOG, OCT4, SSEA1, and SOX2) and 500 μm (AP). Nuclei were stained with DAPI.

All pooled data are represented as means ± SD. The asterisks indicate statistical significance by t test analysis (n.s., not significant; *p < 0.05; **p < 0.01). See also Figure S2.

12 days. Finally, doxycycline was removed in the last 4 days, and iPSC colonies were analyzed at day 16, by counting the NANOG-positive (NANOG$^+$) colonies (Figure 2A). The number of NANOG$^+$ colonies was strongly reduced after both *Tcf1* and *β-catenin* silencing, with respect to the control (Figures 2B, S2C, and S2D). Furthermore, the few colonies that were formed after *Tcf1* silencing were very small and with little NANOG expression (Figure 2C). In contrast, shScr-derived iPSCs formed with high efficiency, were positive to alkaline phosphatase (AP), expressed stem cell markers (such as SSEA-1, NANOG, OCT4, SOX2, *Sall1*, and *Rex1*), and differentiated into all three germ layers (Figures 2D S2E, and S2F). Finally, to exclude adaptation of the MEFs to the loss of *Tcf1*, we infected MEFs with shTcf1A and used doxycyline to induce the four factors at the same time. Also, in this case, we observed a decrease in the NANOG$^+$ colonies, although this effect was weaker, as the MEFs were not hygromycin selected (Figure S2G). These data show that continuous silencing of *β-catenin* or *Tcf1* for 16 days impairs reprogramming efficiency.

## Inhibition of the Wnt Pathway during the Early Phases Enhances MEF Reprogramming via TCF1 Activity

As TCF1 did not appear to have any role in the maintenance of ESC self-renewal, we hypothesized that TCF1 might control reprogramming onset, i.e., the early steps of the process. Thus, we investigated *Tcf1* expression at different time points after doxycycline induction.

THY1 can be followed as an early marker of reprogramming (Brambrink et al., 2008; Stadtfeld et al., 2008). Cells negative for the expression of this marker 3 days after four-factor induction are enriched in the population undergoing reprogramming (Polo et al., 2012). So four-factor MEFs were induced with doxycycline and sorted by fluorescence-activated cell sorting (FACS) 3, 6, and 9 days after induction for the presence or absence of THY1 (Figures 3A and S3A). Enrichment of *Thy* expression in sorted cells was confirmed by real-time PCR (Figure S3B). Cells undergoing reprogramming embark into MET (Esteban et al., 2012; Li et al., 2010; Samavarchi-Tehrani et al., 2010). Thus, we analyzed expression of epidermal markers, *Epcam* and *Cdh1*, and mesenchymal markers, *Snai1*, *Slug*, and *Vimentin* (ten Berge et al., 2008). We observed, as previously shown (Polo et al., 2012), that THY1-negative cells undergo efficient MET, as they upregulated *Epcam* and *Cdh1* and downregulated *Snai1*, *Slug*, and *Vimentin*. In contrast, THY1-positive cells maintained the mesenchymal phenotype (Figure 3B). In addition, the senescence genes *p21*, *p16*, and *p19*, which have been shown to be a barrier to the reprogramming of MEFs into iPSCs (Banito et al., 2009; Hong et al., 2009; Kawamura et al., 2009; Li et al., 2009; Marión et al., 2009; Utikal et al., 2009), were downregulated in the THY1-negative cells (Figure 3B). Finally, the THY1-negative cells gave rise to fully reprogrammed

iPSCs colonies, whereas the THY1-positive cells did not (Figure 3C).

We found that, while in the THY1-negative cells, *Tcf3* expression remained almost constant at all time points of the reprogramming process, it increased from 6 to 9 days in the THY1-positive cells. This indicates that as expected, cells undergoing reprogramming indeed maintain low levels of Tcf3, the repressor of pluripotency (Lluis et al., 2011). In contrast, *Tcf1* expression levels increased progressively from 0 to 6 days in both THY1-positive and THY1-negative cells, before decreasing again in both populations 9 days postinduction (pi) (Figure 3D).

*Tcf1* has several isoforms, including full-length and ΔN isoforms (*FLTcf1* and Δ*NTcf1*, respectively), which have been extensively studied (Reya and Clevers, 2005; Van de Wetering et al., 1996). ΔNTCF1 was shown to be a repressor, as it lacks the β-catenin binding domain (Roose et al., 1999; Waterman, 2004). We therefore investigated which *Tcf1* isoform increases during reprogramming of MEFs. FLTCF1 was greatly increased 6 days pi, as seen using an antibody against FLTCF1 (Figure 3E). FLTCF1 is also the isoform that is expressed in ESCs. In contrast, ΔNTCF1, which is highly expressed in thymocytes (Ioannidis et al., 2001; Yu et al., 2010), was not detected during the reprogramming process (Figure 3E).

Although the expression profile of *Tcf1* was similar in the THY1-positive and THY1-negative cells 6 days pi, the activation of the Wnt signaling pathway was different. Activation of the Wnt pathway, through analysis of the 7TGC reporter activity (Fuerer and Nusse, 2010), was higher in the THY1-positive cells with respect to the THY1-negative cells (Figure 3F). Furthermore, expression of the Wnt/β-catenin targets *CyclinD1*, *Axin2*, and *BMP4* was increased in the THY1-positive cells with respect to the THY1-negative cells, with a peak at 6 days pi (Figure 3G), indicating that Wnt activity is much higher in the THY1-positive cells, which do not undergo reprogramming.

To confirm these observations, we analyzed β-catenin levels in THY1-positive and THY1-negative cells at 6 days pi. Here, active and total β-catenin accumulated more in the THY1-positive cells, clearly indicating that β-catenin can efficiently activate the pathway along with TCF1 in the THY1-positive cells only (Figures 3H and S3C). In contrast, in the THY1-negative cells, Tcf1 appeared to act as a repressor, as at 6 days postinduction, the Wnt pathway was inactive and β-catenin accumulated much less than in the THY1-positive cells (Figure 3H). Indeed, when β-catenin does not accumulate, TCF1 acts as a repressor, by binding to corepressor factors, such as members of the Groucho-related family (Reya et al., 2003; Roose et al., 1998).

To further investigate the repressive activity of TCF1, we overexpressed *Tcf1* in MEFs and analyzed target genes. In particular, for this purpose, we overexpressed *FLTcf1*, which increased during reprogramming, and as a control, *ΔNTcf1*. *Axin2* was drastically downregulated after both *ΔNTcf1* and *FLTcf1* expression respect to the empty vector (E.V.), which indicated that both isoforms repress the Wnt signaling pathway (Figure 4A). The repressive activity of TCF1 was converted into an activation of the Wnt pathway when Chiron, a GSK3 inhibitor, or Wnt3a were added to the *FLTcf1* infected MEFs. *Axin2* was upregulated upon pathway activation (Figures S4A and S4B).

We observed that the mesenchymal genes *Vim*, *Slug*, and *Snai1* were downregulated by overexpression of both isoforms of *Tcf1* (Figure 4A). The senescence genes are upregulated in ESCs that express very high levels of β-catenin, resulting in an impairment of cell-fusion-mediated reprogramming (Lluis et al., 2010). Therefore, we analyzed their expression after *Tcf1* upregulation. *p21*, *p19*, and *p16* were all downregulated upon *FLTcf1* and Δ*NTcf1* overexpression (Figure 4A). In contrast, senescence genes and *Snai1* do not change in their expression when the Wnt pathway is activated in shTcf1A-MEFs (Figure S4C). Finally, to determine whether TCF1 directly regulates MET and senescence genes, we performed chromatin immunoprecipitation (ChIP) assays in MEFs, which demonstrated binding of TCF1 to *Snai1*, *p21*, and *Axin2* promoters (Figure 4B).

Overall, these data indicated that TCF1 can act as a repressor of the Wnt/β-catenin pathway in MEFs, and this results in the repression of some of the mesenchymal and senescent genes.

Next, we investigated whether overexpression of *Tcf1* increased the number of cells undergoing reprogramming. Indeed, we observed a higher number of THY1-negative cells 6 days after infection of four-factor MEFs, compared to EV. (Figure 4C). Also, these cells showed downregulation of *Axin2* as well as the mesenchymal genes *Vim*, *Snai1*, and *Slug* and the senescence markers *p19* and *p21* (Figure 4D).

Next, because *Tcf1* increased 6 days pi, we investigated further whether perturbation of *Tcf1* at this time point was essential in the reprogramming process. For this purpose, we infected four-factor MEFs with shTcf1A, shTcf1B, and shScr, selected with hygromycin, induced with doxycycline, FACS sorted the THY1-negative cells 6 days after induction, and plated these cells in equal numbers (Figure 4E). We observed a reduction in the number of $NANOG^+$ clones from the shTcf1-infected MEFs when compared to the control (Figures 4F and S4D). This shows that silencing the repressive activity of *Tcf1* in THY1-negative cells inhibits the reprogramming process.

To determine whether this effect was dependent on the activation of the MET and/or senescence genes, we analyzed gene expression 6 days after induction in the THY1-negative cells. Interestingly, there was an upregulation of the mesenchymal gene *Snai1* and a downregulation

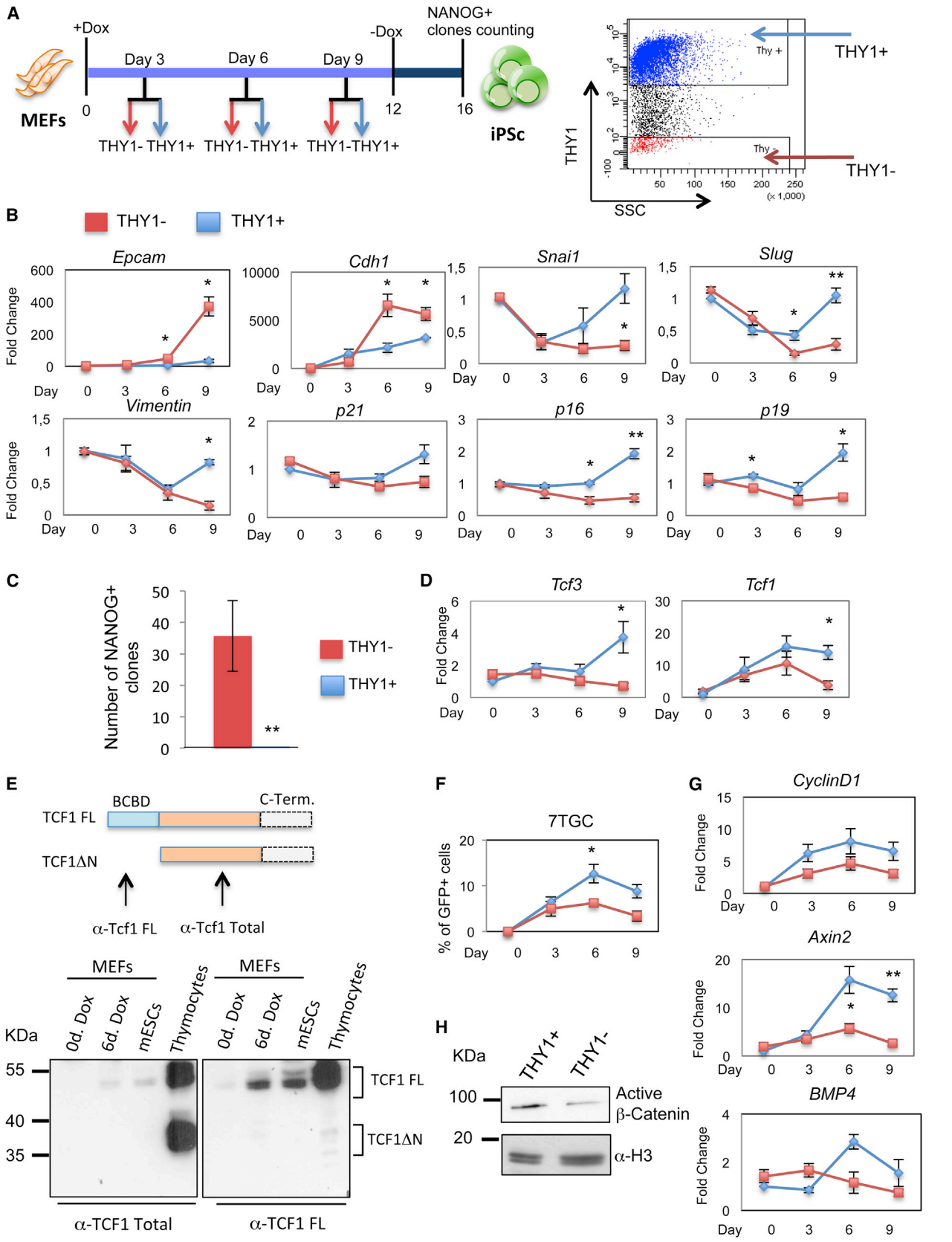


*(legend on next page)*

of the epithelial genes *Cdh1* and *Epcam* (Figure 4G). Moreover, *p21* and *p16* were upregulated 6 days pi in the shTcf1-infected MEFs (Figure 4G). These data indicate that silencing the repressive activity of TCF1 in the THY1-negative cells in the early phases of reprogramming blocks MET and increases senescence barrier.

### Wnt "Off" State Is an Early Reprogramming Marker

To further monitor whether Wnt "off" cells in early reprogramming phases embark upon efficient reprogramming, we infected four-factor MEFs with a lentivirus carrying the 7xTcf-eGFP reporter (7TGC) for TCF/β-catenin activity and *mCherry* under the constitutive SV40 promoter (Figure S5A) (Fuerer and Nusse, 2010). Among the cells that were mCherry positive, four populations of cells with different GFP fluorescence levels were FACS sorted 6 days after doxycycline induction (Figures 5A and S5B). *Axin2* was analyzed to separate these populations of sorted cells accordingly to the Wnt activity (Figure S5B). $GFP^+$ and $GFP^-$ cells (fractions P5 and P6), which had the Wnt pathway "on" and "off," respectively, were analyzed for the expression of pluripotency and for MET and senescent genes. As expected, *Axin2*, *CyclinD1*, and *BMP4* were more expressed in the $GFP^+$ cells than in $GFP^-$ cells. The $GFP^-$ cells underwent efficient MET, as they upregulated *Epcam* and *Cdh1* and expressed low levels of *Snai1*, *Vimentin*, and *Slug* with respect to $GFP^+$ cells. Also, the senescent gene *p16* and *p19* were downregulated in $GFP^-$ cells. Furthermore, the pluripotency markers *Rex1*, *Nanog*, *Oct4*, and *Sall1* were efficiently expressed in $GFP^-$ cells (Figure 5B). Finally, when replated and cultured in presence of doxycycline, only $GFP^-$ cells formed a very high number of $NANOG^+$ or $AP^+$ clones, whereas $GFP^+$ cells did not (Figures 5C, S5C, and S5D). We also analyzed $GFP^+$ cells using immunofluorescence and showed that these cells expressed Nestin (Figure 5D), which suggested they were more differentiated. These results clearly indicate that in the initial steps of the reprogramming process, i.e., up to 6 days after doxycycline induction, the Wnt "off" state is a robust marker of reprogramming.

To further confirm these data, we treated four-factor MEFs for different times with IWP2, an inhibitor of Wnt secretion (Figure 5E) (ten Berge et al., 2011). IWP2 treatment for the first 6 days decreased *Tcf1* expression and increased *Tcf3* expression in the whole-cell population. Along with its effects on Wnt secretion, this resulted in inhibition of the activation of the Wnt/β-catenin pathway, as demonstrated by the repression of *Axin2* (Figure 5F). Together with IWP2, doxycycline induction was applied for 12 days, and the iPSC colonies were analyzed at day 16 (4 days after doxycycline removal) (Figure 5E). MEFs treated with IWP2 for 6 days expressed high levels of *Nanog*, *Rex1*, and endogenous *Oct4* (Figure 5F). Furthermore, the number of iPSC colonies was strongly increased when MEFs were treated for the first 3 or 6 days with IWP2 (Figure 5G). In addition, the silencing of *p21* after IWP2 treatment for 6 days did not result in an increase of reprogramming, further confirming that p21 is an important effector of the Wnt pathway inhibition in the reprogramming process (Figures S5E and S5F). In contrast,

**Figure 3. Time-Dependent Activation of Wnt/β-Catenin Pathway Controls Reprogramming of Four-Factor-Induced MEFs**

(A) Experimental scheme of time course analysis of FACS-sorted cells. Four-factor MEFs were induced with doxycycline as in Figure 2A. At days 3, 6, and 9, the cells were FACS-sorted for THY1-positive ($THY1^+$; blue) and THY1-negative ($THY1^-$; red) expression (right panel) and analyzed.

(B) Time-dependent expression of MET and senescence markers. Relative expression of epithelial markers (*Epcam*, *Cdh1*), mesenchymal markers (*Snai1*, *Slug*, and *Vimentin*), and senescent markers (*p21*, *p16*, and *p19*) in THY1-positive (blue) and THY1-negative (red) sorted cells (n = 3 independent experiments).

(C) An equal number of THY1-positive (blue) and THY1-negative (red) cells were sorted and plated on feeders at day 6 after doxycycline induction. The number of reprogrammed clones was analyzed using NANOG immunostaining (n = 3 independent experiments).

(D) Expression of *Tcf3* and *Tcf1* was analyzed in sorted THY1-positive (blue) and THY1-negative (red) cells using quantitative real-time PCR at the indicated days after doxycycline induction (n = 3 independent experiments).

(E) Schematic representation of the two main TCF1 isoforms. TCF1FL contains a N-terminal β-catenin binding domain (BCBD), whereas TCF1ΔN lacks this domain. Representative western blotting of four-factor MEF extracts on day 0 and day 6 after doxycycline induction. Extracts from ESCs and thymocytes were used as controls. Antibodies against the total TCF1 isoforms and against the full-length TCF1 were used.

(F) MEFs were infected with 7TGP reporter construct and induced with doxycycline as in Figure 2A. At days 3, 6, and 9, the cells were analyzed by GFP expression by FACS (n = 3 independent experiments).

(G) Expression of Wnt/β-catenin target genes (*Axin2*, *CyclinD1*, and *BMP4*) were analyzed in sorted THY1-positive (blue) and THY1-negative (red) cells using quantitative real-time PCR at the indicated days after doxycycline induction (n = 3 independent experiments).

(H) Representative western blot of active β-catenin in nuclear extracts of THY1-positive and THY1-negative sorted cells 6 days after doxycycline induction.

All pooled data are represented as means ± SD. The asterisks indicate statistical significance by t test analysis (* $p < 0.05$; ** $p < 0.01$). See also Figure S3.

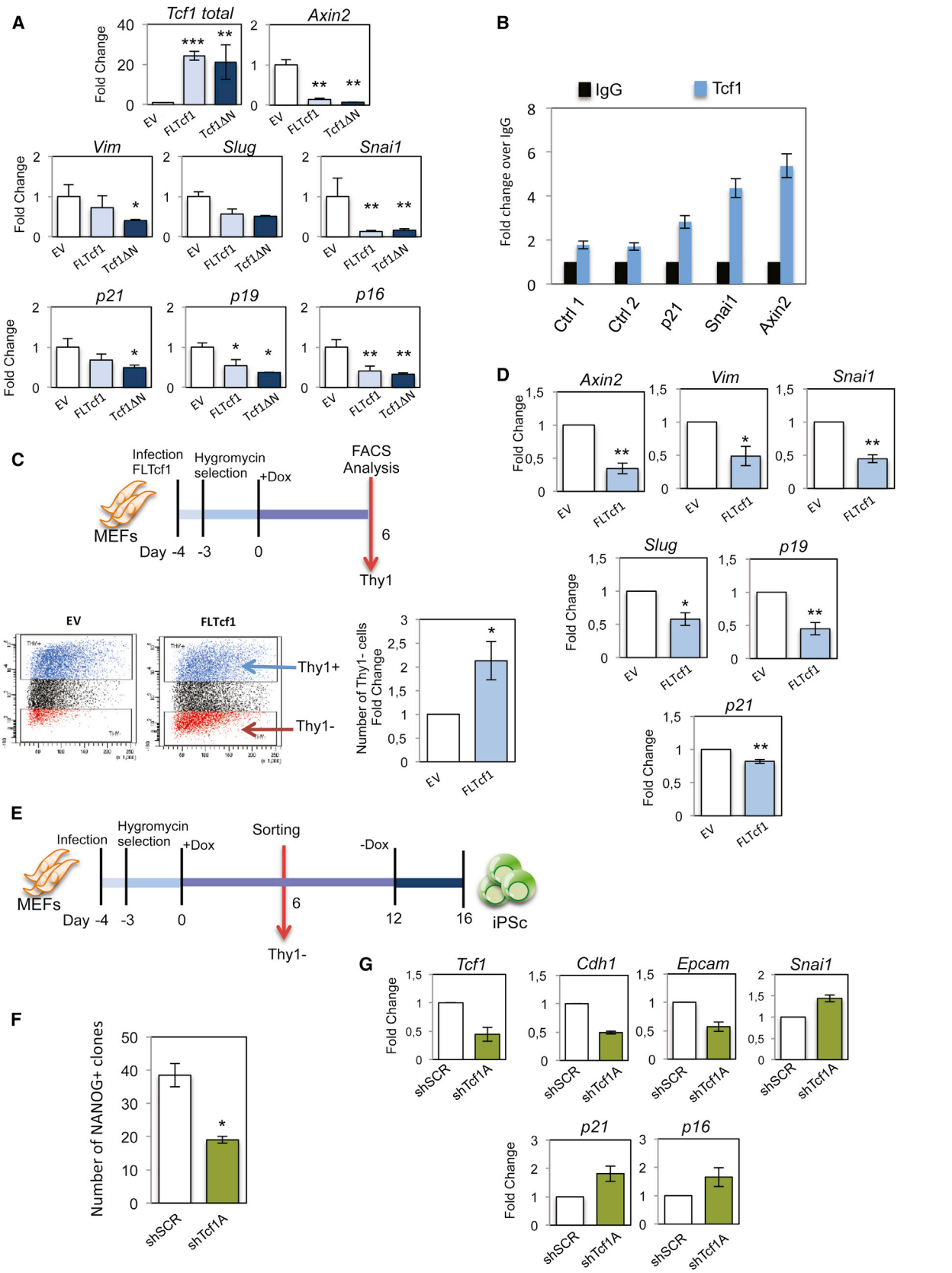


(legend on next page)

treatment of IWP2 from day 6 to day 12 or continuous inhibition of the Wnt pathway with IWP2 strongly reduced the reprogramming efficiency (Figure 5G). This indicated that the pathway should be inhibited during the first phase of reprogramming and should have a basal activation level during the second phase of reprogramming. To confirm these data, we transfected MEFs with shTcf1 (Figure S5G). In this way, we obtained that shTcf1 was lost within 6 days after induction (Figure S5H), whereas in the infected cells, the silencing was constant for all the reprogramming process (Figures S5J and S5K). We found that whereas the constant inhibition of *Tcf1* resulted in a decreased number of NANOG$^+$ colonies (Figure 2B), *Tcf1* transient inhibition resulted in increased efficiency of reprogramming (Figure S5I).

Activation of the pathway by adding Wnt3a early during the reprogramming process inhibits its efficiency (Figures 5G and S5L), whereas the addition of Wnt3a late during the reprogramming process only resulted in a slight increase in the reprogramming efficiency (Figure 5G). In addition, the combined inhibition and activation with IWP2 and Wnt3a during the early and late phases of reprogramming, respectively, moderately increased the efficiency of reprogramming as compared to early inhibition alone (Figure 5G). This indicates that inhibition of Wnt signaling in the early phase is essential and that a basal activation of Wnt pathway is sufficient during late phases of the reprogramming process (Figure 5G). Finally, we used two additional inhibitors of the Wnt pathway to treat the MEFs during early reprogramming phases: Dkk1, which acts as Wnt ligand antagonist (Katoh and Katoh, 2007; Niida et al., 2004), and ICRT3, which blocks the interaction between β-catenin and T cell factors (Faunes et al., 2013; Gonsalves et al., 2011). We further confirmed that early inhibition of the pathway results in increased reprogramming efficiency (Figure S5L). Overall, these findings showed that time-dependent perturbation of the Wnt pathway is fundamental to enhance reprogramming efficiency.

## DISCUSSION

Earlier we showed that cyclic activation of the Wnt signaling pathway is necessary to enhance cell-fusion-mediated reprogramming (Lluis et al., 2008). Also, we showed that finely tuned levels of the Wnt pathway are essential for enhancing somatic cell reprogramming. Too high or too low levels of β-catenin activity result in an impaired reprogramming efficiency (Lluis et al., 2008). Here, we demonstrate that, to achieve reprogramming, Wnt signaling needs to be repressed during the early phase of the process and to be active at the late steps; indeed, in a recent interesting study, a similar conclusion was reached (Ho et al., 2013). However, whereas Ho et al. studied prevalently the function of TCF3 in the regulation of reprogramming and focused on the analysis of the whole MEFs population, here we have extensively studied the function of TCF1, demonstrating its essential role during the reprogramming process. In addition, we have characterized the activity of TCF1 in the THY-negative cells, which are the cells that undergo reprogramming. We have shown that TCF1 acts as a repressor of the Wnt signaling pathway at the onset of reprogramming. Furthermore, it promotes repression of senescent genes and activation of MET (by inhibition of transcription of mesenchymal genes and by activation of epidermal genes) in the THY-negative cells, whereas TCF1 acts as an activator in the THY-positive cells that do not undergo reprogramming.

**Figure 4. TCF1 Is a Repressor of Senescent and Mesenchymal during the First Days of Reprogramming**

(A) Four-factor MEFs were infected with lentiviruses overexpressing either *FLTcf1* or *ΔN-Tcf1*. Infected cells were selected with hygromycin. Four days after infection, the expression of Wnt/β-catenin pathway target (*Axin2*), mesenchymal markers (*Vimentin*, *Slug*, and *Snai1*), and senescence markers (*p21*, *p19*, and *p16*) were analyzed (n = 3 independent experiments). EV, empty vector control.

(B) Quantitative ChIP assay of the TCF1 targets *Axin2*, *Snai1*, and *p21* in the four-factor MEFs. ChIP was performed using rabbit immunoglobulin G or a specific antibody against TCF1 (n = 2 independent experiments).

(C) Four-factor MEFs were infected with lentivirus overexpressing *FLTcf1* or with an empty vector (EV) and selected with hygromycin. Six days after doxycycline induction, cells were analyzed by THY1 expression by FACS (n = 3 independent experiments).

(D) Quantitative real-time PCR expression analysis of empty vector (EV) or *FLTcf1*-overexpressing cells at 6 days after doxycycline induction (n = 3 independent experiments).

(E) Experimental scheme: four-factor MEFs were infected and treated as in Figure 2A. THY1-negative cells (THY1$^-$) were sorted at day 6 after doxycycline induction, as indicated.

(F) The same number of THY1-negative cells was sorted at day 6 after doxycycline induction of shScr or shTcf1A-infected four-factor MEFs and plated on feeders. The number of NANOG$^+$ clones was determined under each treatment (n = 3 independent experiments).

(G) Quantitative real-time PCR expression analysis of shScr and shTcf1A-infected, THY1$^-$, four-factor MEFs at day 6 after doxycycline induction. The mesenchymal (*Snai1*),; epithelial (*Cdh1*, *Epcam*), and senescence (*p21*, *p16*) genes are analyzed (n = 2 independent experiments).

All pooled data are represented as means ± SD. The asterisks indicate statistical significance by t test analysis (* $p < 0.05$; ** $p < 0.01$). See also Figure S4.

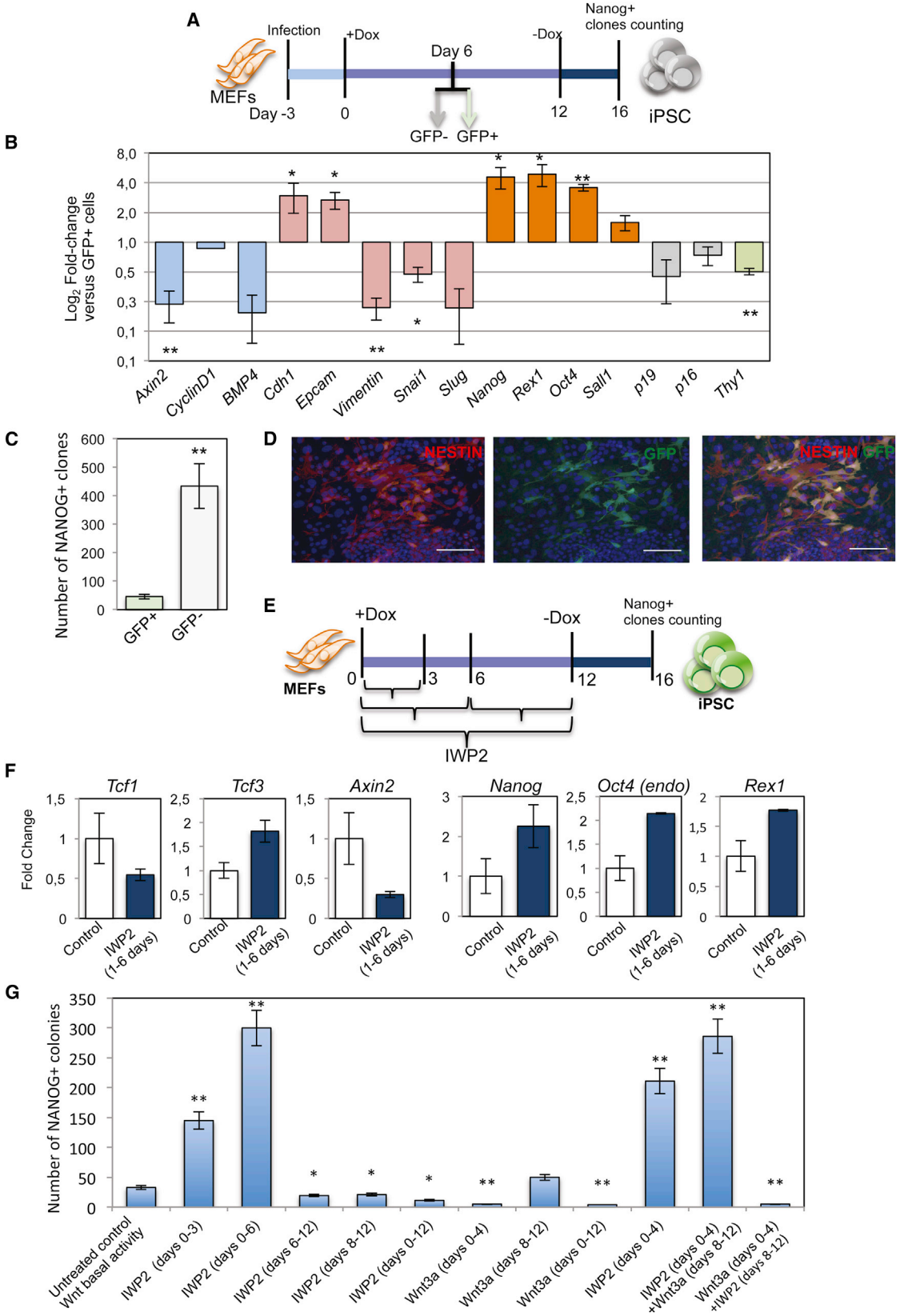


(legend on next page)

Of note, during the reprogramming process, THY-positive cells represent the majority of the total cell population; therefore, the repressive activity of TCF1 in the THY-negative cells cannot be identified without isolating them.

Finally, by sorting the "Wnt-off" cells, we obtained a striking increase in the number of reprogrammed NANOG$^+$ clones, thus clearly identifying the "Wnt-off" state as an early reprogramming marker.

It is interesting to note how different the roles of TCF3 and TCF1 are in the control of somatic cell reprogramming. We showed previously that deletion of *Tcf3* induces increased AcH3 and a decreased number of H3K9me3 heterochromatin foci. These epigenome modifications ultimately enhance reprogramming efficiency (Lluis et al., 2011). Here, we showed that the role of TCF1 during the early reprogramming phase is correlated with the repression of senescence genes and with the activation of MET. Ho et al. (2013) provided evidence that TCF3 and TCF4 promote early reprogramming events by repressing Wnt pathway target genes, including TCF1 and LEF1. However, they also postulated that TCF3 and TCF4 could control other targets that are independent of TCF1 and LEF1 or of the Wnt pathway activation (Ho et al., 2013). It is tempting to speculate that the latter mentioned might be activated by the epigenetic modifications induced by *Tcf3* derepression.

Very little is known about TCF1 activity in ESCs, although it has been demonstrated that in medium lacking LIF, TCF1 contributes to the effect of Wnt3a stimulation to ESC self-renewal (Yi et al., 2011). Here, we have revealed that in medium containing LIF and serum, wild-type ESCs and ESCs silenced for *Tcf1* do not show differences in self-renewal and differentiation, indicating that TCF1 does not control either process. TCF1 is instead a key regulator of the reprogramming process. This led to the interesting observation that some key transcription factors do not always control both somatic cell reprogramming processes and ESC self-renewal, as the effects on these two processes can be distinct.

Both MET and the downregulation of senescence genes are essential processes to achieve somatic cell reprogramming (Esteban et al., 2012; Mahmoudi and Brunet, 2012). Our data show that TCF1 is an important regulator of these processes. Senescent cells are characterized by cell-cycle arrest due to p16$^{INK4a}$ induction. Cell proliferation is crucial in the reprogramming process, and thus cell-cycle arrest is a major barrier to the efficiency of this process. Indeed, mouse fibroblasts cannot be reprogrammed efficiently when two antiproliferative genes, *p16$^{INK4a}$* and *p19$^{ARF}$*, which are part of the *Ink4/Arf* locus, are highly expressed. Accordingly, silencing of the *Ink4/Arf* locus restores reprogramming efficiency in senescent cells. Furthermore, knockdown of *p53* and *p21* also accelerates reprogramming of human and mouse fibroblasts (Banito et al., 2009; Hong et al., 2009; Kawamura et al., 2009; Li et al., 2009; Marión et al., 2009; Utikal et al., 2009). Thus, senescence is a barrier to the reprogramming activity, and this can be overcome by TCF1 action, which maintains low expression of *p21* and *p19* during reprogramming.

During MET, SOX2, OCT4, and C-MYC have been shown to supress *Snai1* and TGF-β signaling, whereas KLF4 has been shown to upregulate *E-cadherin* (Li et al., 2010; Samavarchi-Tehrani et al., 2010). Here, we found that TCF1 activity is correlated not only with repression of senescence genes, but also with MET activation. Embryoid bodies derived from ESCs undergo epithelial-to-mesenchymal transition in a Wnt-dependent process, with the Wnt activity inducing upregulation of *Snai1* and repression of *E-cadherin* (ten Berge et al., 2008). It is therefore intriguing that during reprogramming, TCF1 enhances MET

**Figure 5. Inhibition of the Wnt/β-Catenin Pathway during the First Days of the Reprogramming Process Increases Reprogramming Efficiency**

(A) Four-factor MEFs were infected with lentiviruses carrying 7TGP reporter. GFP$^+$ and GFP$^-$ cells were sorted 6 days after doxycycline induction. Doxycycline was removed at day 12, and colonies were analyzed at day 16.

(B) GFP$^+$ and GFP$^-$ cells were sorted 6 days pi and analyzed by quantitative real-time PCR for the indicated markers (n = 3 independent experiments).

(C) The number of NANOG-positive clones in GFP$^+$- and GFP$^-$-sorted cells at day 16 (n = 3 independent experiments).

(D) GFP$^+$ cells were FACS-sorted at day 6 pi, and cells were analyzed by immunofluorescence for the expression of Nestin. Representative images of the immunofluorescence are shown. Scale bars, 100 μm.

(E) Experimental scheme: four-factor MEFs were treated with doxycycline for 12 days and with IWP2 to inhibit Wnt secretion for the indicated days. At day 16, after doxycycline removal, the colonies were stained for NANOG expression and counted.

(F) Four-factor MEFs were treated with IWP2 for 6 days. Quantitative real-time PCR of control and treated cells (n = 3 independent experiments).

(G) The number of NANOG-positive clones in the control and four-factor MEFs treated with IWP2 for the first 3, 4, 6, or 12 days or for the intervals from 6 to 12 or 8 to 12 days as indicated, Wnt3a for the first 4 or 12 days or for the intervals from 8 to 12 days as indicates, or with combination of IWP2 and Wnt3a at the indicated times (n = 3 independent experiments).

All pooled data are represented as means ± SD. The asterisks indicate statistical significance by t test analysis (n.s., not significant; * $p < 0.05$; ** $p < 0.01$). See also Figure S5.

by transcriptionally repressing *Vim*, *Slug*, and *Snai1* and upregulating *E-cadherin*. Furthermore, we observed that TCF1 directly represses *Snai1* by binding to its promoter. SNAI1 has been shown to be a transcriptional repressor of *E-cadherin* (Batlle et al., 2000). Thus, it might well be that *E-cadherin* is derepressed as a consequence of TCF1-mediated repression of Snai1.

However, we cannot definitively conclude here what the prevalent role of TCF1 is during reprogramming, i.e., if the main function of TCF1 is to modulate senescence genes and MET or also to activate other factors downstream of the Wnt pathway. Finally, it will be particularly interesting to investigate if the Wnt "off" state mediated by the repressive activity of TCF1 is one of the most efficient early reprogramming markers.

## EXPERIMENTAL PROCEDURES

### iPSC Induction

The reprogramming experiments were routinely conducted in gelatinized plates, in the ESC culture medium supplemented with 2 μg/ml doxycycline, as described in Carey et al. (2010). Briefly, after doxycycline withdrawal, the cultures were grown in the ESC medium supplemented with 15% FBS. Colonies with ESC morphology were picked 4–6 days after doxycycline withdrawal and grown as iPSC colonies on a feeder layer of MEFs that was inactivated with mitomycin C.

### Virus Preparation and MEF Infection

Lentiviruses were packaged in HEK293T cells. Briefly, the HEK293T cells were cultured in Dulbecco's modified Eagle's medium supplied with 10% FBS (Life Technologies), 10 U/ml penicillin, 10 μg/ml streptomycin, 2 mM glutamine, 1 mM sodium pyruvate, and 1 × nonessential amino acids. For the transfection, $5 \times 10^6$ HEK293T cells were seeded onto 10 cm plates and transfected with 10 μg pLKO-shTcf1A, pLKO-shTcf1B, or pLKO-shScr, 6.5 μg pCMV-dR8.9 dvpr, and 3.5 μg pCMV-VSV-G packaging plasmids. After 48 and 72 hr, the supernatants were collected and centrifuged at 20,000 rpm for 1.5 hr at 20°C. The pellet with the viruses was resuspended in PBS (Life Technologies) and stored at −80°C.

For the reprogramming experiments, $2 \times 10^5$ MEFs were infected with either pLKO-shTcf1A, pLKO-shTcf1B, or pLKO-shScr in the MEF culture medium. After 48 hr, hygromycin selection (20 μg/ml) was applied for 3–4 days. For iPSC induction, the cells were then plated in equal numbers ($5 \times 10^4$) onto gelatin-coated six-well plates in the ESC culture medium supplemented with 2 μg/ml of doxycycline.

All animal procedures were approved by the local ethics committee, and met the guidelines of the local and European regulations.

## SUPPLEMENTAL INFORMATION

Supplemental Information includes five figures, two tables, and Supplemental Experimental Procedures, and can be found with this article online at http://dx.doi.org/10.1016/j.stemcr.2014.04.001.

## AUTHOR CONTRIBUTIONS

F.A., I.T., L.O., F.L., and M.P.C. planned the experiments; F.A., I.T., L.O., and F.L. performed research and acquired the data; F.A., I.T., L.O., F.L., and M.P.C. analyzed data; F.L. and M.P.C. supervised the project; and M.P.C. wrote the paper.

## ACKNOWLEDGMENTS

We would like to thank Karthik Arumugam, Lucia Marucci, and Elisa Pedone for critically reading the manuscript; Bruno Di Stefano for suggestions to iPSC generation experiments; and Vanessa Chigancas and Neus Romo for technical support. We thank Luigi Naldini for providing lentiviral vectors, Hans Clevers for providing the *Tcf1* constructs, and Rudolf Jaenisch for providing the inducible four-factor mouse model. We are grateful for support from an European Research Council grant (242630-RERE) (to M.P.C.), an HFSP grant (to M.P.C.), the Ministerio de Ciencia e Inovación (SAF2011-28580) (to M.P.C.), Fundacio' La Marato' de TV3 (to M.P.C.), the AXA Research Fund (to M.P.C.), the "Miguel Servet" Project of the Instituto de Salud Carlos III (CP10/00445) (to F.L.), the Ministerio de Ciencia e Innovación FPI (to F.A.), and the Ingenium ITN Marie Curie Program (to I.T.). We acknowledge support of the Spanish Ministry of Economy and Competitiveness, "Centro de Excelencia Severo Ochoa 2013-2017" (SEV-2012-0208).

Received: June 24, 2013
Revised: April 4, 2014
Accepted: April 7, 2014
Published: May 6, 2014

## REFERENCES

Banito, A., Rashid, S.T., Acosta, J.C., Li, S., Pereira, C.F., Geti, I., Pinho, S., Silva, J.C., Azuara, V., Walsh, M., et al. (2009). Senescence impairs successful reprogramming to pluripotent stem cells. Genes Dev. *23*, 2134–2139.

Batlle, E., Sancho, E., Francí, C., Domínguez, D., Monfar, M., Baulida, J., and García De Herreros, A. (2000). The transcription factor snail is a repressor of E-cadherin gene expression in epithelial tumour cells. Nat. Cell Biol. *2*, 84–89.

Brambrink, T., Foreman, R., Welstead, G.G., Lengner, C.J., Wernig, M., Suh, H., and Jaenisch, R. (2008). Sequential expression of pluripotency markers during direct reprogramming of mouse somatic cells. Cell Stem Cell *2*, 151–159.

Brantjes, H., Roose, J., van De Wetering, M., and Clevers, H. (2001). All Tcf HMG box transcription factors interact with Groucho-related co-repressors. Nucleic Acids Res. *29*, 1410–1419.

Cadigan, K.M., and Liu, Y.I. (2006). Wnt signaling: complexity at the surface. J. Cell Sci. *119*, 395–402.

Carey, B.W., Markoulaki, S., Beard, C., Hanna, J., and Jaenisch, R. (2010). Single-gene transgenic mouse strains for reprogramming adult somatic cells. Nat. Methods *7*, 56–59.

Cole, M.F., Johnstone, S.E., Newman, J.J., Kagey, M.H., and Young, R.A. (2008). Tcf3 is an integral component of the core regulatory circuitry of embryonic stem cells. Genes Dev. *22*, 746–755.

Daniels, D.L., and Weis, W.I. (2005). Beta-catenin directly displaces Groucho/TLE repressors from Tcf/Lef in Wnt-mediated transcription activation. Nat. Struct. Mol. Biol. *12*, 364–371.

Esteban, M.A., Bao, X., Zhuang, Q., Zhou, T., Qin, B., and Pei, D. (2012). The mesenchymal-to-epithelial transition in somatic cell reprogramming. Curr. Opin. Genet. Dev. *22*, 423–428.

Faunes, F., Hayward, P., Descalzo, S.M., Chatterjee, S.S., Balayo, T., Trott, J., Christoforou, A., Ferrer-Vaquer, A., Hadjantonakis, A.K., Dasgupta, R., and Arias, A.M. (2013). A membrane-associated β-catenin/Oct4 complex correlates with ground-state pluripotency in mouse embryonic stem cells. Development *140*, 1171–1183.

Fuerer, C., and Nusse, R. (2010). Lentiviral vectors to probe and manipulate the Wnt signaling pathway. PLoS ONE *5*, e9370.

Gonsalves, F.C., Klein, K., Carson, B.B., Katz, S., Ekas, L.A., Evans, S., Nagourney, R., Cardozo, T., Brown, A.M., and DasGupta, R. (2011). An RNAi-based chemical genetic screen identifies three small-molecule inhibitors of the Wnt/wingless signaling pathway. Proc. Natl. Acad. Sci. USA *108*, 5954–5963.

Hikasa, H., Ezan, J., Itoh, K., Li, X., Klymkowsky, M.W., and Sokol, S.Y. (2010). Regulation of TCF3 by Wnt-dependent phosphorylation during vertebrate axis specification. Dev. Cell *19*, 521–532.

Ho, R., Papp, B., Hoffman, J.A., Merrill, B.J., and Plath, K. (2013). Stage-specific regulation of reprogramming to induced pluripotent stem cells by Wnt signaling and T cell factor proteins. Cell Rep. *3*, 2113–2126.

Hong, H., Takahashi, K., Ichisaka, T., Aoi, T., Kanagawa, O., Nakagawa, M., Okita, K., and Yamanaka, S. (2009). Suppression of induced pluripotent stem cell generation by the p53-p21 pathway. Nature *460*, 1132–1135.

Hoppler, S., and Kavanagh, C.L. (2007). Wnt signalling: variety at the core. J. Cell Sci. *120*, 385–393.

Hurlstone, A., and Clevers, H. (2002). T-cell factors: turn-ons and turn-offs. EMBO J. *21*, 2303–2311.

Ioannidis, V., Beermann, F., Clevers, H., and Held, W. (2001). The beta-catenin—TCF-1 pathway ensures CD4(+)CD8(+) thymocyte survival. Nat. Immunol. *2*, 691–697.

Kalluri, R., and Weinberg, R.A. (2009). The basics of epithelial-mesenchymal transition. J. Clin. Invest. *119*, 1420–1428.

Katoh, M., and Katoh, M. (2007). WNT signaling pathway and stem cell signaling network. Clin. Cancer Res. *13*, 4042–4045.

Kawamura, T., Suzuki, J., Wang, Y.V., Menendez, S., Morera, L.B., Raya, A., Wahl, G.M., and Izpisúa Belmonte, J.C. (2009). Linking the p53 tumour suppressor pathway to somatic cell reprogramming. Nature *460*, 1140–1144.

Kühl, S.J., and Kühl, M. (2013). On the role of Wnt/β-catenin signaling in stem cells. Biochim. Biophys. Acta *1830*, 2297–2306.

Li, H., Collado, M., Villasante, A., Strati, K., Ortega, S., Cañamero, M., Blasco, M.A., and Serrano, M. (2009). The Ink4/Arf locus is a barrier for iPS cell reprogramming. Nature *460*, 1136–1139.

Li, R., Liang, J., Ni, S., Zhou, T., Qing, X., Li, H., He, W., Chen, J., Li, F., Zhuang, Q., et al. (2010). A mesenchymal-to-epithelial transition initiates and is required for the nuclear reprogramming of mouse fibroblasts. Cell Stem Cell *7*, 51–63.

Lluis, F., and Cosma, M.P. (2009). Somatic cell reprogramming control: signaling pathway modulation versus transcription factor activities. Cell Cycle *8*, 1138–1144.

Lluis, F., Pedone, E., Pepe, S., and Cosma, M.P. (2008). Periodic activation of Wnt/beta-catenin signaling enhances somatic cell reprogramming mediated by cell fusion. Cell Stem Cell *3*, 493–507.

Lluis, F., Pedone, E., Pepe, S., and Cosma, M.P. (2010). The Wnt/β-catenin signaling pathway tips the balance between apoptosis and reprograming of cell fusion hybrids. Stem Cells *28*, 1940–1949.

Lluis, F., Ombrato, L., Pedone, E., Pepe, S., Merrill, B.J., and Cosma, M.P. (2011). T-cell factor 3 (Tcf3) deletion increases somatic cell reprogramming by inducing epigenome modifications. Proc. Natl. Acad. Sci. USA *108*, 11912–11917.

MacDonald, B.T., Tamai, K., and He, X. (2009). Wnt/beta-catenin signaling: components, mechanisms, and diseases. Dev. Cell *17*, 9–26.

Mahmoudi, S., and Brunet, A. (2012). Aging and reprogramming: a two-way street. Curr. Opin. Cell Biol. *24*, 744–756.

Marión, R.M., Strati, K., Li, H., Murga, M., Blanco, R., Ortega, S., Fernandez-Capetillo, O., Serrano, M., and Blasco, M.A. (2009). A p53-mediated DNA damage response limits reprogramming to ensure iPS cell genomic integrity. Nature *460*, 1149–1153.

Marson, A., Foreman, R., Chevalier, B., Bilodeau, S., Kahn, M., Young, R.A., and Jaenisch, R. (2008). Wnt signaling promotes reprogramming of somatic cells to pluripotency. Cell Stem Cell *3*, 132–135.

Merrill, B.J., Pasolli, H.A., Polak, L., Rendl, M., García-García, M.J., Anderson, K.V., and Fuchs, E. (2004). Tcf3: a transcriptional regulator of axis induction in the early embryo. Development *131*, 263–274.

Moon, R.T., Kohn, A.D., De Ferrari, G.V., and Kaykas, A. (2004). WNT and beta-catenin signalling: diseases and therapies. Nat. Rev. Genet. *5*, 691–701.

Murry, C.E., and Keller, G. (2008). Differentiation of embryonic stem cells to clinically relevant populations: lessons from embryonic development. Cell *132*, 661–680.

Niida, A., Hiroko, T., Kasai, M., Furukawa, Y., Nakamura, Y., Suzuki, Y., Sugano, S., and Akiyama, T. (2004). DKK1, a negative regulator of Wnt signaling, is a target of the beta-catenin/TCF pathway. Oncogene *23*, 8520–8526.

Ombrato, L., Lluis, F., and Cosma, M.P. (2012). Regulation of self-renewal and reprogramming by TCF factors. Cell Cycle *11*, 39–47.

Pereira, L., Yi, F., and Merrill, B.J. (2006). Repression of Nanog gene transcription by Tcf3 limits embryonic stem cell self-renewal. Mol. Cell. Biol. *26*, 7479–7491.

Polo, J.M., Anderssen, E., Walsh, R.M., Schwarz, B.A., Nefzger, C.M., Lim, S.M., Borkent, M., Apostolou, E., Alaei, S., Cloutier, J., et al. (2012). A molecular roadmap of reprogramming somatic cells into iPS cells. Cell *151*, 1617–1632.

Reya, T., and Clevers, H. (2005). Wnt signalling in stem cells and cancer. Nature *434*, 843–850.

Reya, T., Duncan, A.W., Ailles, L., Domen, J., Scherer, D.C., Willert, K., Hintz, L., Nusse, R., and Weissman, I.L. (2003). A role for Wnt

signalling in self-renewal of haematopoietic stem cells. Nature *423*, 409–414.

Roose, J., Molenaar, M., Peterson, J., Hurenkamp, J., Brantjes, H., Moerer, P., van de Wetering, M., Destrée, O., and Clevers, H. (1998). The Xenopus Wnt effector XTcf-3 interacts with Groucho-related transcriptional repressors. Nature *395*, 608–612.

Roose, J., Huls, G., van Beest, M., Moerer, P., van der Horn, K., Goldschmeding, R., Logtenberg, T., and Clevers, H. (1999). Synergy between tumor suppressor APC and the beta-catenin-Tcf4 target Tcf1. Science *285*, 1923–1926.

Samavarchi-Tehrani, P., Golipour, A., David, L., Sung, H.K., Beyer, T.A., Datti, A., Woltjen, K., Nagy, A., and Wrana, J.L. (2010). Functional genomics reveals a BMP-driven mesenchymal-to-epithelial transition in the initiation of somatic cell reprogramming. Cell Stem Cell *7*, 64–77.

Sato, N., Meijer, L., Skaltsounis, L., Greengard, P., and Brivanlou, A.H. (2004). Maintenance of pluripotency in human and mouse embryonic stem cells through activation of Wnt signaling by a pharmacological GSK-3-specific inhibitor. Nat. Med. *10*, 55–63.

Silva, J., Barrandon, O., Nichols, J., Kawaguchi, J., Theunissen, T.W., and Smith, A. (2008). Promotion of reprogramming to ground state pluripotency by signal inhibition. PLoS Biol. *6*, e253.

Sokol, S.Y. (2011). Maintaining embryonic stem cell pluripotency with Wnt signaling. Development *138*, 4341–4350.

Stadtfeld, M., Maherali, N., Breault, D.T., and Hochedlinger, K. (2008). Defining molecular cornerstones during fibroblast to iPS cell reprogramming in mouse. Cell Stem Cell *2*, 230–240.

Tam, P.P., and Loebel, D.A. (2009). Specifying mouse embryonic germ cells. Cell *137*, 398–400.

Tam, W.L., Lim, C.Y., Han, J., Zhang, J., Ang, Y.S., Ng, H.H., Yang, H., and Lim, B. (2008). T-cell factor 3 regulates embryonic stem cell pluripotency and self-renewal by the transcriptional control of multiple lineage pathways. Stem Cells *26*, 2019–2031.

Tanaka, S.S., Kojima, Y., Yamaguchi, Y.L., Nishinakamura, R., and Tam, P.P. (2011). Impact of WNT signaling on tissue lineage differentiation in the early mouse embryo. Dev. Growth Differ. *53*, 843–856.

ten Berge, D., Koole, W., Fuerer, C., Fish, M., Eroglu, E., and Nusse, R. (2008). Wnt signaling mediates self-organization and axis formation in embryoid bodies. Cell Stem Cell *3*, 508–518.

ten Berge, D., Kurek, D., Blauwkamp, T., Koole, W., Maas, A., Eroglu, E., Siu, R.K., and Nusse, R. (2011). Embryonic stem cells require Wnt proteins to prevent differentiation to epiblast stem cells. Nat. Cell Biol. *13*, 1070–1075.

Utikal, J., Polo, J.M., Stadtfeld, M., Maherali, N., Kulalert, W., Walsh, R.M., Khalil, A., Rheinwald, J.G., and Hochedlinger, K. (2009). Immortalization eliminates a roadblock during cellular reprogramming into iPS cells. Nature *460*, 1145–1148.

van Amerongen, R., and Nusse, R. (2009). Towards an integrated view of Wnt signaling in development. Development *136*, 3205–3214.

Van de Wetering, M., Castrop, J., Korinek, V., and Clevers, H. (1996). Extensive alternative splicing and dual promoter usage generate Tcf-1 protein isoforms with differential transcription control properties. Mol. Cell. Biol. *16*, 745–752.

Waterman, M.L. (2004). Lymphoid enhancer factor/T cell factor expression in colorectal cancer. Cancer Metastasis Rev. *23*, 41–52.

Willert, K., and Jones, K.A. (2006). Wnt signaling: is the party in the nucleus? Genes Dev. *20*, 1394–1404.

Wray, J., Kalkan, T., Gomez-Lopez, S., Eckardt, D., Cook, A., Kemler, R., and Smith, A. (2011). Inhibition of glycogen synthase kinase-3 alleviates Tcf3 repression of the pluripotency network and increases embryonic stem cell resistance to differentiation. Nat. Cell Biol. *13*, 838–845.

Yi, F., Pereira, L., and Merrill, B.J. (2008). Tcf3 functions as a steady-state limiter of transcriptional programs of mouse embryonic stem cell self-renewal. Stem Cells *26*, 1951–1960.

Yi, F., Pereira, L., Hoffman, J.A., Shy, B.R., Yuen, C.M., Liu, D.R., and Merrill, B.J. (2011). Opposing effects of Tcf3 and Tcf1 control Wnt stimulation of embryonic stem cell self-renewal. Nat. Cell Biol. *13*, 762–770.

Yu, Q., Sharma, A., and Sen, J.M. (2010). TCF1 and beta-catenin regulate T cell development and function. Immunol. Res. *47*, 45–55.

**Stem Cell Reports, Volume *2***

**Supplemental Information**

# Temporal Perturbation of the Wnt Signaling Pathway in the Control of Cell Reprogramming Is Modulated by TCF1

**Francesco Aulicino, Ilda Theka, Luigi Ombrato, Frederic Lluis, and Maria Pia Cosma**

# Inventory of Supplemental Information

1) Supplemental Figures
    a. Figure S1: *Tcf1* Knock-down in mouse ESCs (related to figure 1).
    b. Figure S2: *Tcf1* Knock-down in MEFs (related to figure 2).
    c. Figure S3: FACS-Sorting Controls (related to figure 3)
    d. Figure S4: Regulation of Wnt pathway by *Tcf1* in MEFs (related to figure 4).
    e. Figure S5: Temporal inhibition of Wnt pathway increases cell reprogramming (related to figure 5).

2) Supplemental Experimental Procedures: A detailed description of all the experimental procedures used in this work.

3) Supplemental Tables
    a. Table S1: Antibodies used with corresponding dilutions.
    b. Table S2: Short hairping and Primer sequences

** **Supplementary figures**

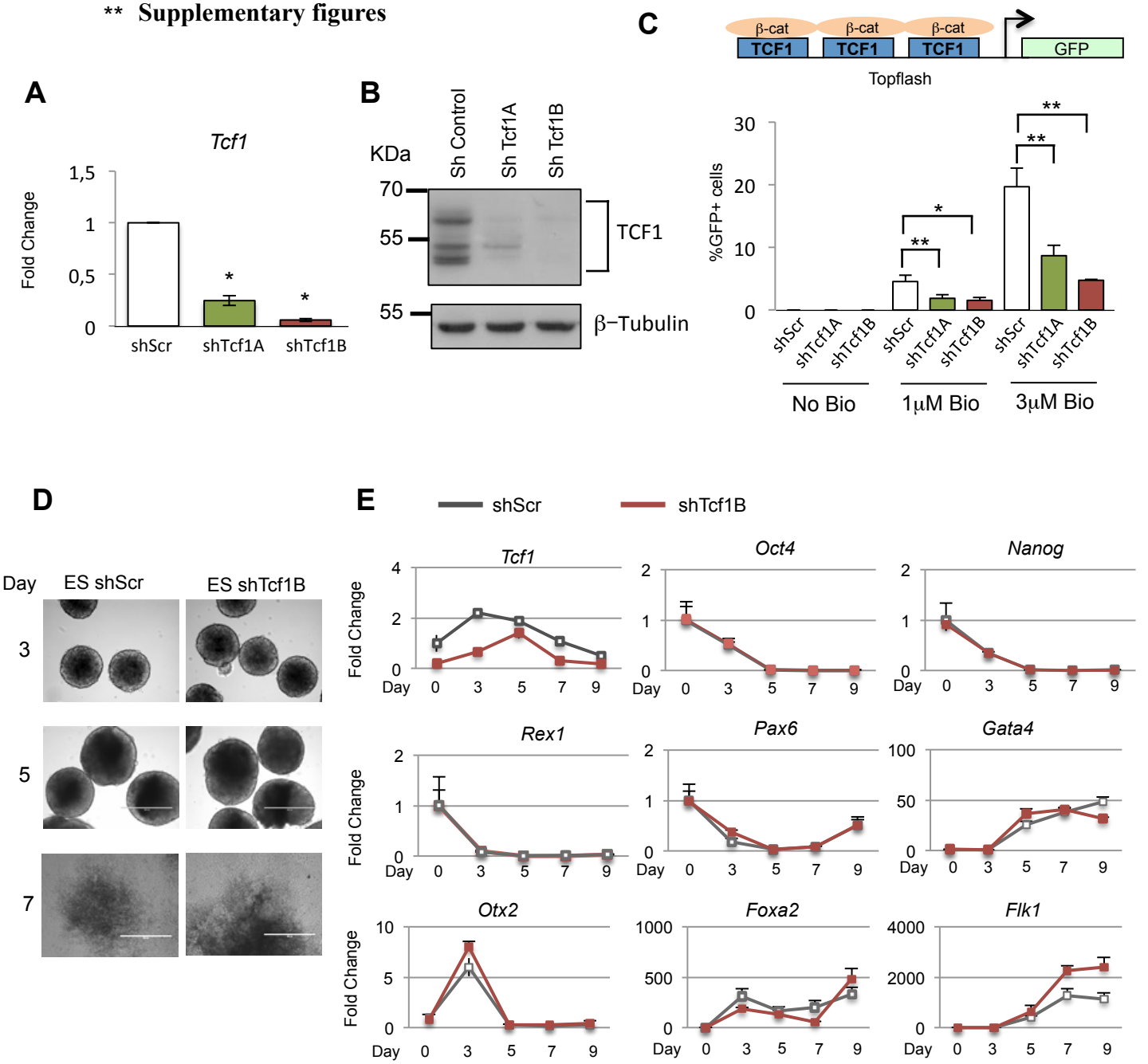


**Supplementary Figure S1. Tcf1 knock-down in mouse ESCs.**
ESCs were infected with pLKO lentivirus carrying scrambled (shScr) or *Tcf1* silencing (shTcf1A and shTcf1B). Infected cells were selected using hygromycin. **(A)** Quantitative PCR analysis; (n = 3 independent experiments ). **(B)** Representative Western blot (as indicated). **(C)** shScr, shTcf1A and shTcf1B ES cells were infected with 7TGP reporter and selected for stable incorporation. Cells were then treated with BIO at indicated concentrations during 24h to activate the Wnt/β-catenin pathway. Number of GFP+ cells was mesured by FACS analysis; (n=4 independent experiments) **(D)** ESCs-shScr and ESCs-shTcf1B were subjected to differentiation through aggregation into embryoid bodies. Representative phase-contrast images at 3, 5, and 7 days during embryoid body differentiation. Scale bar: 400μm. **(E)** Representative qRT-PCR experiment (out of two independent experiments) for the detection of *Tcf1*, stem-cell (*Oct-4*, *Nanog*, *Rex1*), ectoderm (*Pax6*, *Otx2*), mesoderm (*Flk1*) and endoderm (*Gata4* and *Foxa2*) marker genes in embryoid bodies at different times p.i.. The levels are normalised to *Gapdh*.
All pooled data are represented as means ± SD. The asterisks indicate statistical significance by t test analysis (* $p<0.05$; ** $p<0.01$).

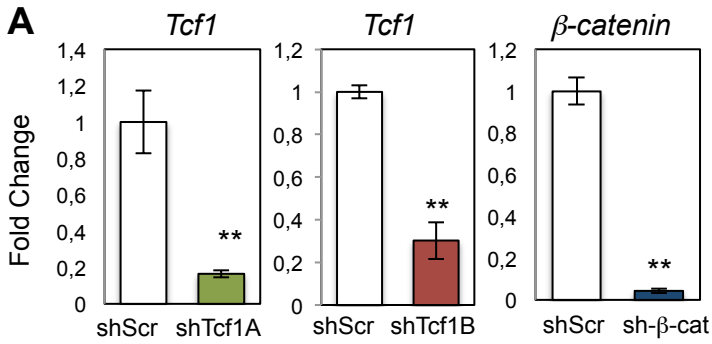


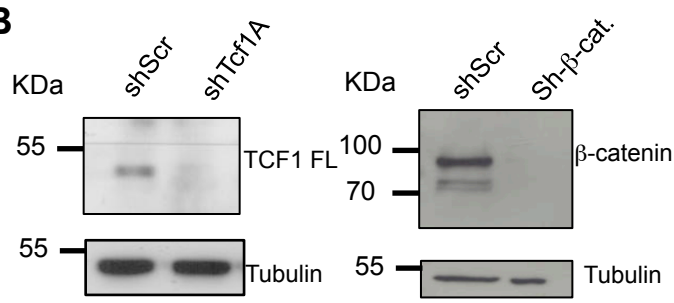


C

| Silencing | Min % | Max % |
|---|---|---|
| **shScr** | 0,0746 | 0,118 |
| **shTcf1A** | 0,014 | 0,046 |
| **shβcat** | 0,01 | 0,03 |

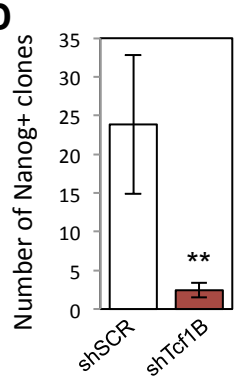


| Infection | Number NANOG+ clones | Efficiencicy (Min-Max %) |
|---|---|---|
| ShScr | **24 ±9** | 0,03-0066 |
| ShTcf1B | **3 ±1** | 0,004-0,008 |

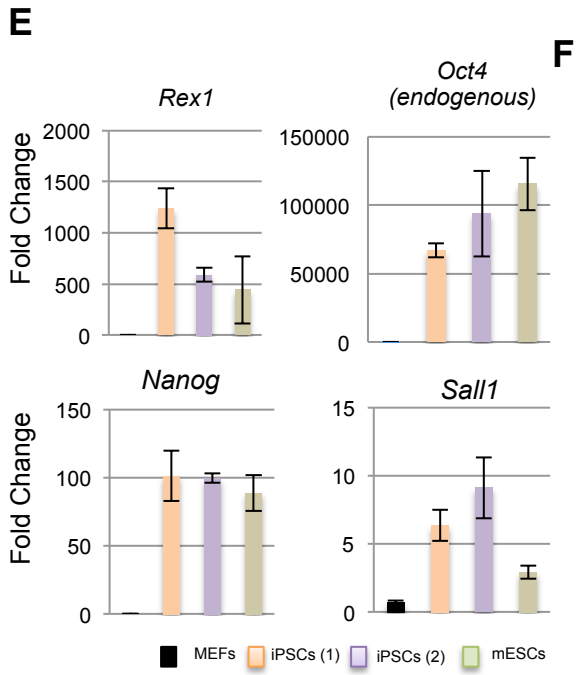


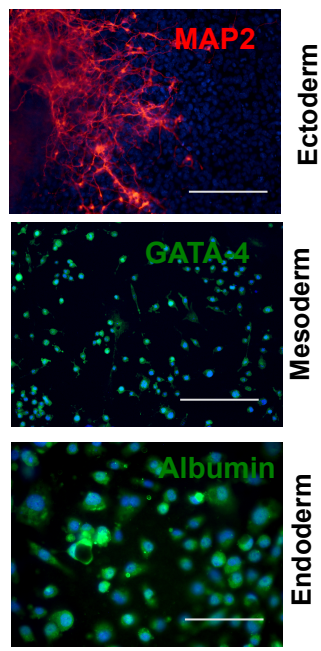


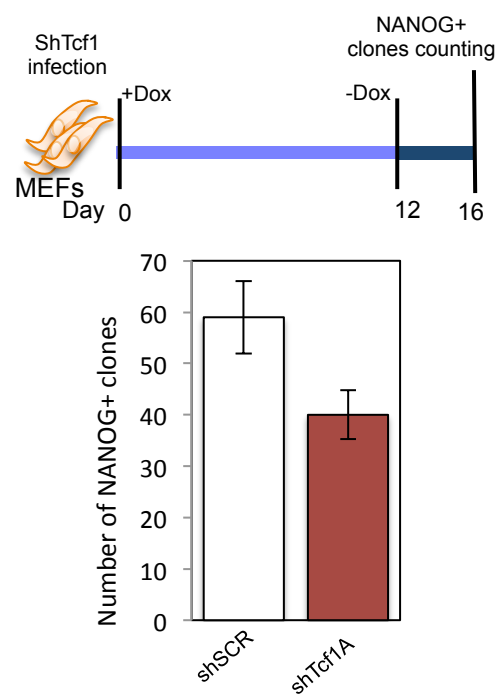


**Supplementary Figure S2. Tcf1 knock-down in MEFs.**

**(A)** Quantitative PCR analysis of *ß-catenin* and *Tcf1* expression in four-factor MEFs infected with shScr, sh-ß-catenin shTcf1A and shTcf1B, as indicated. (n = 3 independent experiments ). **(B)** Representative Western blots showing ß-catenin and FLTCF1 protein levels in the cells infected with shScr, sh-ß-catenin and shTcf1A. **(C)** Table showing minimum and maximum efficiencies of reprogramming in the cells infected with shScr, sh-ß-catenin and shTcf1A. Efficiencies are calculated: Number of NANOG+ clones/ Number of plated MEFs x100. **(D)** Number of NANOG positive (NANOG$^+$) clones obtained in four-factor MEFs infected with shScr and shTcf1B according to each treatment; (n=3 independent experiments ). **(E)** Quantitative RT-PCR analysis of the expression of ESC markers in MEFs, selected iPSC clones, and mouse ESCs. **(F)** Representative images of immunostaining of iPSCs differentiated into ectoderm (MAP2), mesoderm (GATA4) and endoderm (Albumin), as indicated. Scale bars: 200mm **(G)** Number of NANOG positive clones (NANOG+) after Tcf1 silencing without Hygromycin selection (n=2 independent experiments ).

All pooled data are represented as means ± SD. The asterisks indicate statistical significance by t test analysis (* $p<0.05$; ** $p<0.01$).

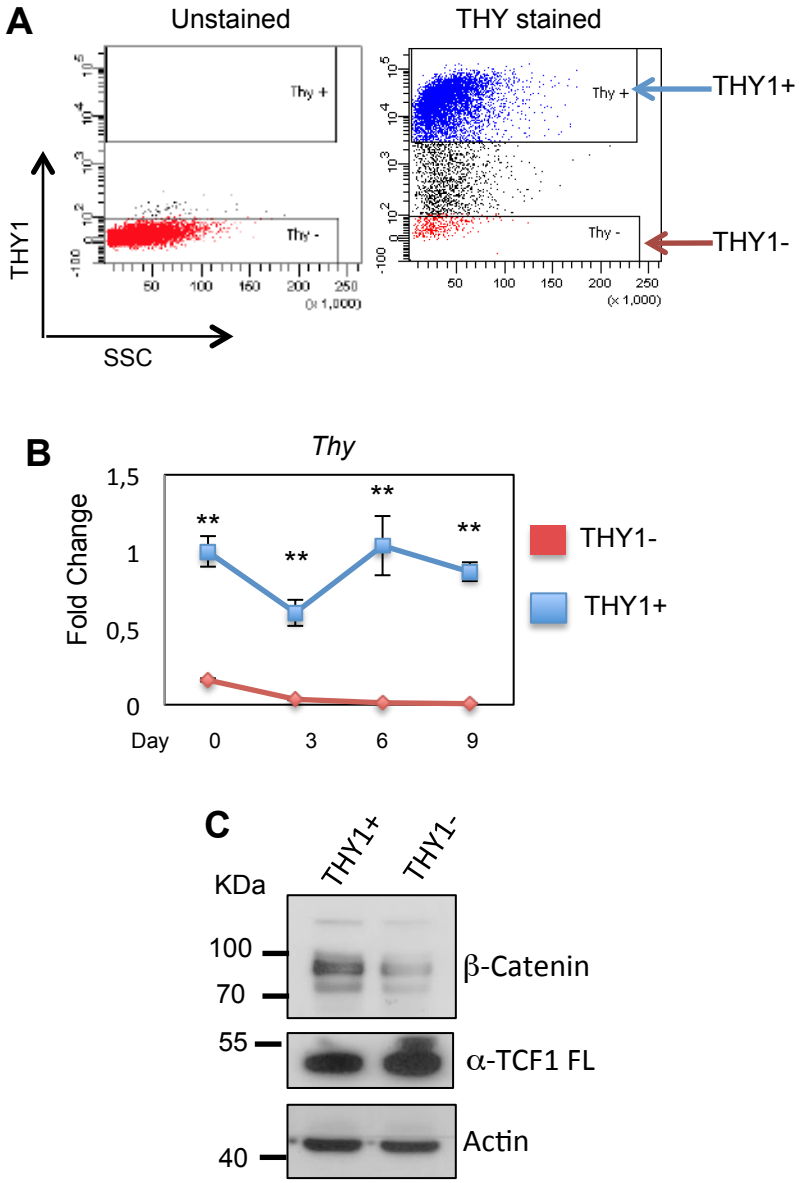


**Supplementary Figure S3.**

**(A)** Four-factor MEFs were induced with doxycycline as in Figure 2A. At days 3, 6 and 9, the cells were FACS-sorted for THY1-positive (THY1$^{+}$; blue) and THY1-negative (THY1$^{-}$; red) expression (right panel), and analysed. Unstained cells were used as negative control (left panel). **(B)** Time-dependent expression of *Thy* in sorted populations (n=3 independent experiments ). **(C)** Representative Western blot of total ß-catenin and TCF1 in THY1-positive and THY1-negative sorted cells 6 days after doxycycline induction.

All pooled data are represented as means ± SD. The asterisks indicate statistical significance by t test analysis (n.s. no significant; * $p<0.05$; ** $p<0.01$).

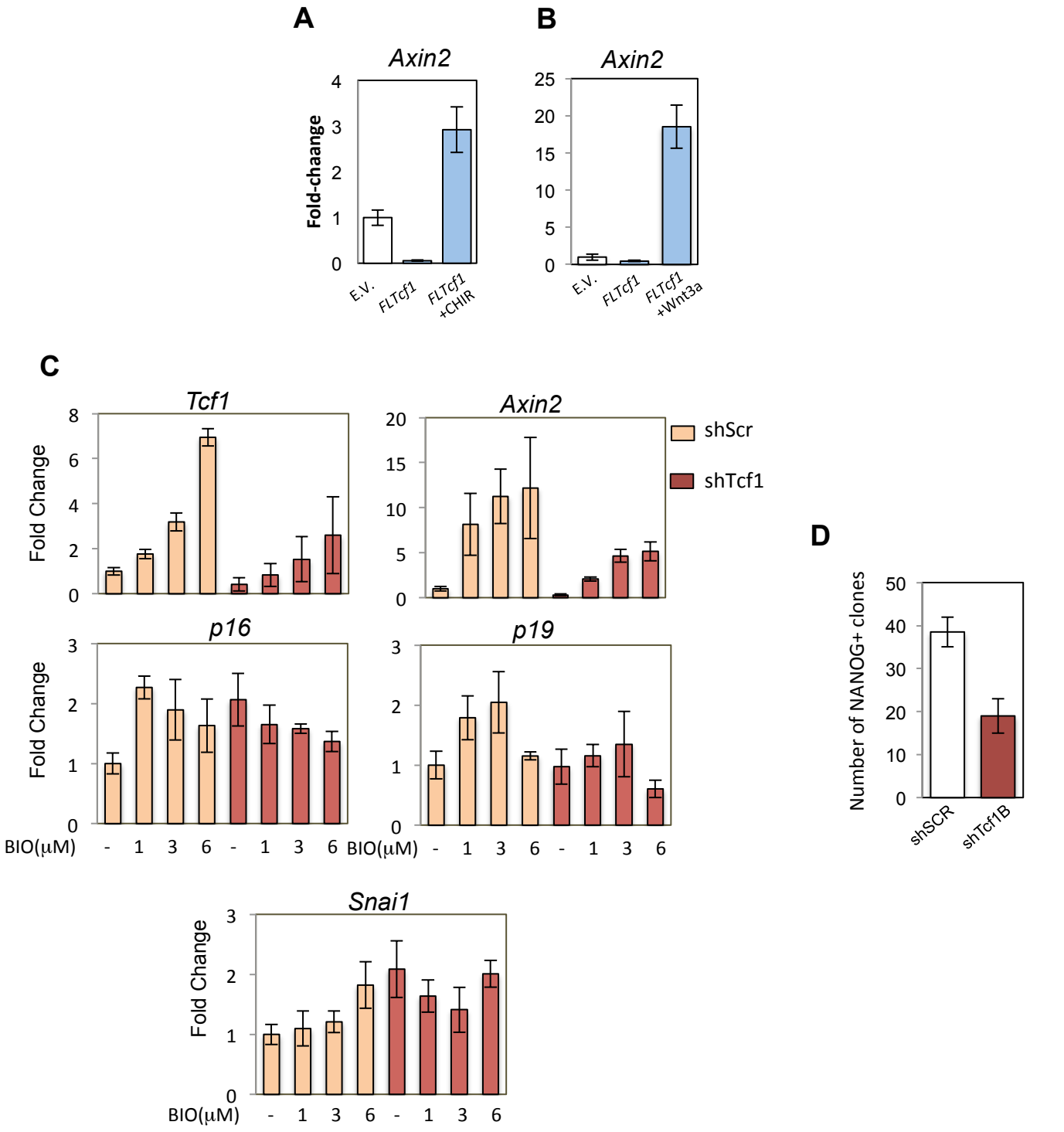


**Supplementary Figure S4.**

**(A,B)** Four-factor MEFs were infected with lentiviruses overexpressing *FLTcf1* and selected with hygromycin. Cells were then treated with Chiron or Wnt3a for 24 hours. qRT-PCR of *Axin2* levels are shown; (n=2 independent experiments ). **(C)** qRT-PCR expression analysis of four-factor MEFs infected with shScr or shTcf1 and treated for 12h with increasing concentrations of Chiron as indicated (N.T.: Non-Treated); (n=2 independent experiments ). **(D)** The same number of THY1-negative cells was sorted at day 6 after doxycycline induction of shScr or shTcf1B-infected four-factor MEFs, and plated on feeders. The number of NANOG+ clones was determined under each treatment; (n = 2 independent experiments ).

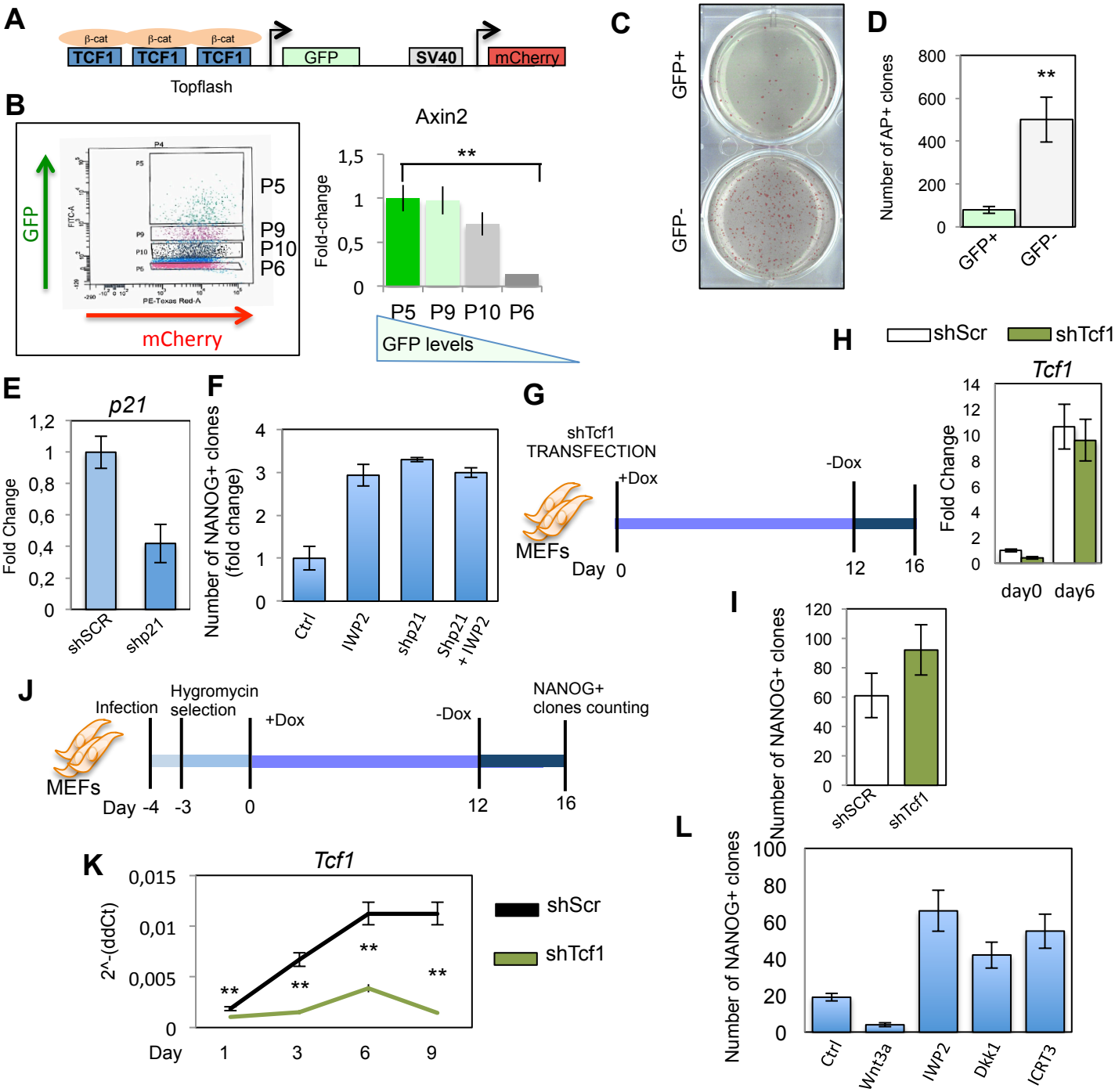


**Figure S5. GFP-negative cells show an increase in the number of AP⁺ iPS colonies**

**(A)** Scheme of 7TGC reporter. **(B)** Cells positive for Cherry expression were sorted by different levels of GFP expression (P5, P9, P10 and P6) at 6 days after doxycycline induction. qRT-PCR of *Axin2* expression is shown; (n=3). **(C)** GFP+ and GFP- cells were sorted at 6 days p.i. and replated on feeders. Doxycicline was removed at day 12. At day 16 plates were stained for Alkaline Phosphatase (AP) staining. **(D)** Quantification of the number of alkaline-phosphatase-positive (AP⁺) colonies at day 16; (n=3 independent experiments). **(E)** Quantitative PCR analysis of *p21*expression in four-factor MEFs infected with shScr and shp21 **(F)** Four-factor MEFs were infected with a lentivirus expressing a silencing for *p21* and cells were treated for 6 days with IWP2. Immunostaining against Nanog was performed, to count the number of reprogrammed clones. (n=2 independent experiments)**(G)** Experimental scheme for iPSCs generation. Four-factor MEFs were transfected with lentiviral vectors carrying shScr or shTcf1. Doxycycline was applied from 0 to 12 days and removed for the following 4 days. Immunostaining against Nanog was performed, to count the number of reprogrammed clones. **(H)** qRT-PCR of *Tcf1* levels at days 0 and 6 after transfection**. (I)** Number of NANOG positive (NANOG⁺) clones obtained according to experimental procedure indicated in (G), as indicated (n=2 independent experiments)). **(J)** Experimental procedure as in Figure 2A. **(K)** qRT-PCR levels of *Tcf1* expression in shScr and shTcf1 at 1, 3, 6 and 9 after doxycycline induction; (n=3 independent experiments). **(L)** Four-factor MEFs were pre-treated for 3 days with indicated treatments before to apply doxycycline for 12 days. The number of NANOG+ clones was determined under each treatment; (n = 2 independent experiments). All pooled data are represented as means ± SD. The asterisks indicate statistical significance by t test analysis (* $p<0.05$; ** $p<0.01$).

***Supplementary Methods***

*Cell culture*

MEFs were established from E13.5 embryos from reprogrammable mice carrying two (ho/ho) copies of the OKSM cassette and the ROSA26-M2rtTA allele (Carey et al, 2010). The embryos were isolated from the uterus and washed in phosphate-buffered saline (PBS). The head and viscera were removed, and the rest of the body was mechanically disaggregated and then incubated in 0.1% trypsin/ 0.1 mM EDTA solution for 30 min, to allow the cells to detach from the extracellular matrix and from each other. The cells were then mechanically disaggregated and plated onto a 15-cm tissue-culture dish and cultured in MEF culture medium: Dulbecco's modified Eagle's medium (DMEM) supplemented with 10% foetal bovine serum (FBS) 10 U/ml penicillin, 10 μg/ml streptomycin, 2 mM glutamine, 1 mM sodium pyruvate, and 1× non-essential amino acids. The MEFs were kept at 37 °C under 5% $CO_2$.

Wnt3a (100ng/ml) and Dkk1 (100ng/ml) were obtained from R&D systems; IWP2 (2μM) was from Stemgent and ICRT3 (25μM) was purchased from Calbiochem.

Mouse ESCs (129/sv) were cultured on gelatin coated-plates in ESC medium: knock-out DMEM supplemented with 15% FBS (Hyclone), 1X non-essential amino acids, 1X GlutaMax, 1X penicillin/ streptomycin, 1X 2-mercaptoethanol and 1,000 U/ml LIF ESGRO (Chemicon). The differentiation medium for the production of embryoid bodies (EBs) consisted of this ESC culture medium without the LIF. The cells were harvested by trypsinisation, counted, and propagated in hanging drops (400 single ESCs/ 30 μl initial drop) for 2 days, before being transferred to 10 $cm^2$ bacterial dishes. On day 5, the embryoid bodies were transferred onto gelatinised p100 dishes always in differentiation medium.

For the iPSC differentiation the reprogrammed clones were detached from the feeder layer of MEFs and EBs were formed in ESC culture medium without LIF as described above. Furthermore, on day 5 the EBs were successively disaggregated and plated onto gelatin-coated dishes in ESC culture medium in absence of LIF, to allow them to differentiate into the three germ layers. For neural differentiation retinoic acid was added to the culture.

*Constructs preparation*

Short hairpins targeting ß-catenin (shß-cat), Tcf1 (shTcf1A, shTcf1B), p21 (shp21) and a short hairpin control (shScr) were cloned into the pLKO.1-Hygro lentiviral vector (Addgene plasmid #24150), following the manufacturer instructions (http://www.addgene.org/tools/protocols/plko/). The oligonucleotides cloned into the pLKO vector were purchased from Sigma-Aldrich. A list of the oligonucleotides used to generate the short hairpins is given in Supplementary Table S2. pCMV-dR8.9 dvpr (Addgene #8455) and pCMV-VSV-G (Addgene #8454) were used as lentiviral packaging constructs. The FLTcf1 (p45 Tcf-B) and ΔN-Tcf1 (p54 Tcf-E) constructs were kindly provided by Hans Clevers (Van de Wetering et al, 1996). Tcf1 constructs were cloned together with the hygromycin-resistance cassette into p1494 lentiviral vectors that were kindly provided by Luigi Naldini. The 7TGP and 7TGC lentiviral reporter were purchased from Addgene (Addgene #24305; #24304) (Fuerer and Nusse, 2010).

*Virus preparation and ESC infection*

For ESC infection, lentiviral particles were produced following the RNA interference Consortium (TRC) instructions for lentiviral particle production and infection in 6-well plates (http://www.broadinstitute.org/rnai/public/). Briefly 5 $\times 10^5$ HEK293T cells/well were seeded in 6-well plates. The day after plating, the cells were co-transfected with 1 µg pLKO-shTcf1A, pLKO-shTcf1B or pLKO-shScr, 750 µg pCMV-dR8.9, and 250 µg pCMV-VSV-G, using Polyfect reagent (Qiagen). The day after transfection, the HEK293T culture medium was substituted with the ESC culture medium. Then 5 $\times 10^5$ ESCs/well were plated onto gelatin-coated 6-well plates the day before transduction. The lentiviral-containing medium was harvested from HEK293T cells at 48, 72 and 96 h after transfection, filtered, and added to the ESC plates. The day after transduction, these ESCs were washed twice in PBS and hygromycin selection (50 µg/ml) was applied.

*Transient transfection of MEF cells*

For a transient silencing of Tcf1 during reprogramming, $1x10^6$ MEF cells were elctroporated with pLKO-shSCR and pLKO-shTcf1A using Amaxa reagent (Amaxa #VPD-1004) following manufacturer's instructions. After nucleofection, $1x10^5$ cells were plated in a 35mm dish.

*Flow cytometry and immunofluorescence*

For analysis and/or sorting of intermediates, cells were trypsinised, washed once in PBS, and resuspended in PBS with 5% FBS. These harvested cells were incubated with antibodies against Thy1.2.2; 0.04 μg antibody per 1 $\times 10^6$ cells (PE, eBioscience) for 20 min, washed twice in PBS plus 5% FBS, and sorted or analysed as indicated. Unstained cells were used as the negative staining control.

For immunocytochemistry, the cells were fixed with 4% paraformaldehyde for 20 min at room temperature, and then washed twice with PBS. These fixed cells were then incubated in blocking solution containing 10% goat serum (Sigma) and 0.1% Triton X-100 (Sigma) for 1 h at room temperature. The cells were then left overnight at 4 °C in blocking solution containing the primary antibody. The next day, the cells were washed three times with PBS and then incubated with the secondary antibody for 1 h at room temperature. The primary antibodies used are given in Supplementary Table S1. Goat anti-mouse IgG, goat anti-rabbit IgG, (1:1000, Life Technologies) conjugated to Alexa Fluor-488 or Alexa Fluor-594 were used as secondary antibodies. Nuclear staining was performed with DAPI (Life Technologies).

*Alkaline phosphatase staining*

Alkaline phosphatase is an enzyme expressed by ESCs and is used as a marker of pluripotency. To evaluate the alkaline phosphatase expression, the cells were fixed in 10% Neutral Formalin Buffer for 15 min at 4°C, and washed three times with distilled water. These fixed cells were then incubated for 45 min at room temperature in 2ml of the staining solution prepared as follows: 0,005g Naphthol AS MX-PO4 (Sigma, N5000), 0,03g Red Violet LB salt (Sigma, F1625), 200 μl N,N-Dimethylformamide (DMF, Fischer Scientific, D1191), 25 ml of Tris-HCl (MW=157.6, pH 8.3, 0.2M), and 25 ml of distilled water. The alkaline-phosphatase-positive cells showed a red colour and were visible under phase-contrast microscopy.

*RNA extraction and quantitative PCR detection of mRNA*

RNA was extracted and purified using RNAeasy kits (QIAGEN), according to the manufacturer instructions. Total RNA was treated with DNAse I (Qiagen) to prevent DNA contamination.

The cDNA was produced with SuperScript II Reverse Transcriptase kits (Life Technologies) starting from 1 μg mRNA. Real-time quantitative PCR reactions from 8,3 ng of cDNA were set up in triplicate using a LightCycler DNA SYBR Green I Master PCR machine (Roche). For oligos sequences see Table S2.

.

*Cell lysis and immunoblotting*

Cells were harvested and washed twice with PBS. Cell lysis was performed on ice for 25 min, in RIPA buffer (150 mM NaCl, 1% Nonidet P40, 0.5% sodium deoxycholate, 0.1% sodium dodecyl sulphate, 50 mM Tris-HCl, pH 8.0) containing a protease inhibitory cocktail (Roche). Insoluble material was pelleted by centrifugation at 16,000× *g* for 3 min at 4 °C. Protein concentrations were determined using the Bradford assay (Bio-Rad). Thirty micrograms extract was mixed with 4× sample buffer (40% glycerol, 240 mM Tris/HCl, pH 6.8, 8% SDS, 0.04% bromophenol blue, 5% β-mercaptoethanol), denatured at 96ºC for 5 minutes, separated by SDS-PAGE, and transferred to nitrocellulose membranes (PROTRAN-Whatman, Schleicher&Schuell). The membranes were blocked with 5% non-fat dry milk in TBS-T for 60 min, incubated with primary antibodies overnight at 4 °C, washed three times with TBS-T for 10 min, incubated with the peroxidase-conjugated secondary antibody (1:2000; Amersham Biosciences) in TBST with 5% non-fat dry milk for 60 min, and washed three times with TBST for 10 min. Immunoreactive proteins were detected using Supersignal West Dura HRP Detection kits (Pierce).

*Chromatin immunoprecipitation assay*

ChIP was carried out as described in (Morey et al, 2012). Briefly, ESCs were trypsinised and crosslinked in 1% formaldehyde for 10 min at room temperature. Crosslinking was quenched with 0.125 M glycine for 5 min. The pelleted cells were lysed in 1 ml ChIP buffer and sonicated for 10 min in a Bioruptor sonicator (Diagenode). The soluble material was quantified using Bradford assays. To immunoprecipitate the transcription factors, 500 μg protein was used. Antibodies

were incubated overnight with the chromatin. The immunocomplexes were recovered with 30 µl protein A or G agarose bead slurries. The immunoprecipitated material was washed three times with low-salt buffer and one time with high-salt buffer. DNA complexes were decrosslinked at 65 °C for 3 h, and the DNA was then eluted in 200 µl water using the PCR purification kit (QIAGEN). Two microliters DNA was used for each qPCR reaction, using SYBR green (Fermentas). For oligos sequences see Table S2.

*Statistical Analysis.*

Averages from three independent experiments were calculated for most of the shown experiments and Student's t-tests were performed for statistical analysis. $p < 0.05$ defined statistical significance.

Supplementary Table 1. Antibodies used in the article with corresponding working dilution.

| Antibodies | Working dilution/ Concentration | Company (Catalog number) |
|---|---|---|
| Mouse monoclonal Antibody (Ab) | | |
| microtubule-associated protein 2 (MAP2) | 1:200 (IF) | Abcam (ab11267) |
| CD90.2 (Thy-1.2) | 0,06 µg x $10^6$cells (IF) | eBioscience (12-0902) |
| β-catenin | 1:500 (WB) | BD (MAB-318) |
| stage-specific embryonic antigen 1 (SSEA-1) | 1:100 (IF) | Santa Cruz Biotechnology (sc- 21701) |
| octamer-binding transcription factor-4 (OCT4) | 1:200 (IF) | Santa Cruz Biotechnology (sc-5279) |
| Nestin | 1:200 (IF) | Abcam (ab6142) |
| Albumin | 1:500 (IF) | Abcam (ab19196-2) |
| Tubulin | 1:2000 (WB) | Sigma (T0198) |
| Actin | 1:2000 (WB) | Abcam (ab8226) |
| Antibodies | Working dilution | Company (Catalog number) |
| Rabbit polyclonal Antibody (Ab) | | |
| GATA-4 | 1:200 (IF) | Abcam (ab61170) |
| SRY-box 2 (SOX2) | 1:500 (IF) | Abcam (ab97959) |
| NANOG | 1:300 (IF) | Calbiochem (#SC1000) |
| GFP | 1:500 (IF) | Santa Cruz Biotechnology (sc-8332) |
| TCF1 FL (C6D9) | 1:1000 (WB) | Cell Signaling (#2203) |
| TCF1 Total (C46C7) | 1:1000 (WB)<br>5 µg (ChIP) | Cell Signaling (#2206) |
| Active β-catenin | 1:500 (WB) | Millipore (#05-665) |